**THIS DOCUMENT REPRESENTS WORK IN PROGRESS.
DESIGN PARAMETERS ARE NOT FINALIZED.
COMMENTS AND QUESTIONS MAY BE DIRECTED TO
ROBERT H. SIEMANN (SLAC) OR ROBERT J. NOBLE (FNAL).**

Technical Design Study

for the

ORION Advanced Accelerator Research Facility

February 2, 2001

Stanford Linear Accelerator Center
Stanford University
Stanford, California 94309

Prepared with support from the U.S. Department of Energy under contracts
DE-AC03-76SFO0515 and DE-AC02-76CHO3000.

Table of Contents

Abstract

This document presents the baseline technical design for the ORION Advanced Accelerator Research Facility at the Stanford Linear Accelerator Center, Stanford University. The central goal of the ORION Project is to establish and operate a user-oriented facility for understanding the physics and developing the technology for future high-energy particle accelerators. The ORION Facility will bring together the needed resources for performing a wide range of experiments and have these available and working. The facility has as its centerpiece the Next Linear Collider Test Accelerator (NLCTA) within End Station B at the SLAC Central Research Yard. That site will be modified with the addition of a new high-brightness photoinjector, its associated drive laser and rf system, a data acquisition control room for experimenters, a user laser room, a staging area for experiment preparation, a low-energy experimental hall supplied with beams up to approximately 60 MeV in energy, and a high-energy hall supplied with beams up to 350 MeV.

“Give me a fulcrum on which to rest, and I will move the Earth.”

- Archimedes (287-212 BC), on the lever and fulcrum

1 Introduction

1.1 Origins and the High-Energy Frontier

Particle physics is addressing fundamental questions of the origin of mass and the observed symmetries in Nature. At the highest energies we see Nature on the smallest of scales, which far from being esoteric, is the foundation upon which the origin of our Universe, stable matter, galaxies, and ultimately life, depends. Particle physics is motivated not just by basic scientific questions, but also by the very human questions regarding our own origins. Historically, these types of questions are answered at the energy frontier, and the exponential growth of center-of-mass energy and fundamental discoveries have gone hand-in-hand. Particle accelerators have become our microscopes to study Nature, and the previous century has seen us peer down to distances nearly one-billionth the size of an atom. Today we are on the verge of profound discoveries in physics that may reveal to us why objects have mass, why matter predominates over antimatter, and even how our Universe was born. Only with higher energy accelerators will we find answers to these questions.

1.2 Inventing the New Microscopes

Since the invention of the first optical microscopes 400 years ago, people have strived to see the building blocks that make up our world. Optical microscopes culminated in the early-twentieth century with the imaging of structures within the living cells of our bodies. To see the smaller objects within our cells, including the chromosomes containing genetic material, the use of visible light was replaced with neutrons and more energetic electrons that could be precisely focused to delve deeper. The technologies of electron microscopy and neutron scattering revolutionized biochemistry permitting us to visualize the precise arrangement of atoms and molecules in our cells. From such knowledge, the molecular basis of our genetic code was discovered.

The techniques for using energetic particles to observe Nature at smaller scales not only revolutionized biology in the past century, but also physics. For all their tremendous size today, it is a humbling thought that high-energy particle accelerators are simply large-scale versions of the electron accelerator that produces the x-rays in our dentist's office, and the radio power sources are very much like those in our microwave ovens. Nature apparently gives us only one simple, scalable technique to accelerate charged particles, and that is to provide an electric field always parallel to the particle's velocity. The way to get to higher energies in a shorter distance is to create higher electric fields. It is interesting to note that we can even calculate the highest electric field that we could ever hope to stably achieve. This is the so-called "Klein Limit" of about 10^{16} V/cm where the energy density becomes so high that spontaneous electron-positron production occurs in vacuum, and the field is quenched. At this electric field, a particle accelerator with a length of roughly one-tenth the Earth-Sun separation could in principle achieve the Planck energy of 10^{28} eV where it is thought quantum gravitational effects and the very fabric of space-time become observable. Such energies seem daunting by today's standards, but it serves to remind us that the road to the high-energy frontier is still a very long and exciting one.

High-energy particle accelerators today are large because our technology only allows us to produce macroscopic, stable electric fields up to about 10^7 V/cm using metallic, electromagnetic cavities. This field is equivalent to applying 0.1 eV over one Angstrom, the size of a neutral atom, and corresponds roughly to the field needed to ionize and hence damage any metallic surface. Beyond the 10^{12} eV energy scale, linear accelerators with extra length needed for focusing will become tens to hundreds of kilometers long and unaffordable to build. To dramatically shorten the length of high-energy accelerators, we must learn to create and control, over macroscopic lengths, electric fields much higher than the present limit.

During the last four decades, many creative ideas have been suggested for producing large electric fields in various media including metals, dielectrics and plasmas. In all cases, one must ultimately use some electromagnetic field mode supported by a media or modified by material boundaries to produce a longitudinal component of the electric field to accelerate particles. In the 1970's it was noted that longitudinal, electron plasma oscillations will support electric fields up to order $n^{1/2}$ V/cm, where n is the electron density in units of cm^{-3}, before wave-breaking and plasma turbulence ensue (Ref. 1). For example, a high-density laboratory plasma with 10^{18} electrons/cm^3 can in principle produce 10^9 V/cm acceleration fields. The advent of high peak-power lasers and intense charged-particle beams able to excite large-amplitude, electromagnetic modes in different media resulted in many small experiments being mounted worldwide during the last twenty years to test novel acceleration concepts. The scientific interest in acceleration topics quickly grew, and since 1982 there has been an Advanced Accelerator Concepts Workshop held every two years, which now attracts two to three hundred participants (Ref. 2).

Advanced accelerator research, with its goal of understanding the physics and developing the technologies for reaching high energies, is essential for the future of high-energy physics. With many new, aggressive acceleration experiments being contemplated by university groups, a state-of-the-art experimental facility with a wide range of electron beam energies, variable bunch length and charge, micron-wavelength laser capability, and laboratory infrastructure is needed. Testing new acceleration concepts rapidly and then turning the concepts into prototypical particle accelerators will require the resources of the national labs teamed with the academic community.

1.3 Goals of the ORION Project

The central goal of the ORION Project is to establish and operate a user-oriented facility for understanding the physics and developing the technology for future high-energy particle accelerators. Experiments usually have both state-of-the-art and conventional components with both being critical for success. Often the conventional components require substantial effort to build, maintain and operate. The ORION Facility will bring together the needed resources for performing a wide range of experiments and have these available and working. Experimenters will be provided electron beams up to about 350 MeV in energy, two experimental beam halls, a user laser room, a staging area, instrumentation, utilities, and a data acquisition room. The experimenters will be able to concentrate on the science of their own experiment, enabling rapid progress.

ORION will also provide a dynamic environment for interactions between experimenters and the efficient use of shared resources for advanced accelerator research. It will become a focus for this field of research with a user community that develops and shares a base of experimental techniques. This will lead to information exchange, evolving collaborations, rapid assessments of concepts, and creative approaches to new opportunities. As with all basic research, there is no way to predict the ultimate outcome. But the progress in any field depends on that most precious of commodities, people. The dynamic environment of ORION will hopefully act as a bridge connecting human imagination to the realization of new high-energy accelerators.

2 Design Considerations

2.1 Overview

A user-oriented facility for advanced accelerator research must efficiently combine the strengths of collaborating universities and national laboratories if rapid progress in this field is to be made. Advanced accelerator experiments usually have both state-of-the-art and conventional components. The ORION Facility will bring together the needed resources for performing a wide range of experiments and have them available and working on schedule. A reliable source of particle beam, well-maintained experimental halls, an assembly area for component staging, and a user-friendly control room for data gathering make up the required infrastructure.

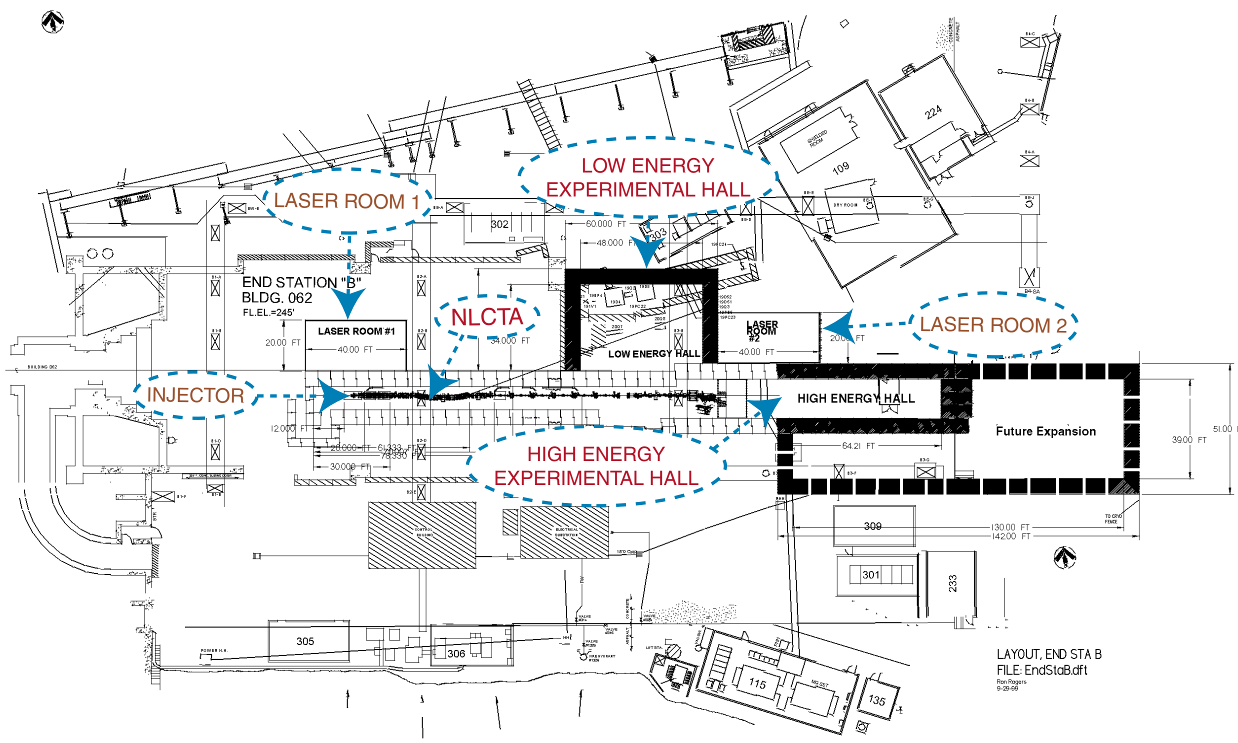

Figure 1. Plan view of the ORION Advanced Accelerator Research Facility at the NLCTA.

To leverage the existing SLAC resources, a number of accelerators and locations on the SLAC site were considered for the new ORION Facility by an internal committee during the summer of 1999. The committee determined that the Next Linear Collider Test Accelerator (NLCTA) (Ref. 3) offered a good opportunity for a user facility with a wide-ranging scientific program. From this study, the basic layout of the ORION Facility originated, as illustrated in

Figure 1 (Ref. 4). The NLCTA would be the centerpiece. It consists of a 60 MeV electron injector and magnetic dipole chicane followed by the main linac, which can accommodate four, 1.8 meter long, X-band (11.4 GHz) accelerating structures. These structures, operating at a conservative 40 MV/m gradient, can increase the beam energy by 288 MeV. The present injector produces a 100 nsec long train of X-band bunches each with about 10^9 electrons. The two natural extraction points for beam to users are at the exit of the chicane following the injector and at the spectrometer magnet at the high-energy end of the NLCTA. A multi-hundred MeV beam for accelerator research would be unique in the world and essential for many aggressive acceleration experiments. A 60-MeV beam is not unique, but having both high and low energies available at the same facility gives breadth to the experimental program and deals with the issue of limited beam availability, making the ORION Facility very attractive. It should be noted that the NLCTA radiation shielding and terminating beam stop were designed for up to 1170 MeV to leave an option for high-energy beam in the future.

The primary role of the NLCTA is to support Next Linear Collider (NLC) development. The NLC development plans for the period 2000 to 2003 call for extensive use of the rf equipment associated with the main linac for prototype testing. High-energy beams may be possible for only limited intervals. However, the injector will be largely unused for NLC development during that period and would be available for other uses. After 2003, multi-hundred MeV beams are expected to be available regularly.

A number of changes and additions are necessary for an NLCTA-based advanced accelerator facility. These include:

- A low-emittance, single (or few) electron-bunch photoinjector to replace the present thermionic source. The thermionic source will be stored for possible future experiments.
- A laser facility to drive the photoinjector.
- A radio-frequency system to power the photoinjector accelerator cells.
- Modern diagnostics, data acquisition system and control system.
- An 800 square-foot room for housing lasers used for the experiments.
- A 1600 square-foot, experimental hall for 7 to 67 MeV beams supplied from the NLCTA injector.
- A 1000 square-foot, experimental hall for 67 to 350 MeV beams supplied from the NLCTA X-band linac sections. Future hall expansion to 5000 square-feet is possible.

2.2 Design Criteria and Beam Requirements

An ORION Workshop was held in February 2000 to elicit input from the potential user community regarding the possible experimental program and the facility's development (Ref. 5). The suggested research program included experiments devoted to advances in plasma and laser-driven accelerators, new experiments in many aspects of beam-plasma interactions, and the development of new beam sources. This Workshop helped to focus the technical outline of the proposed facility.

A combination of the 1999 SLAC faculty study and the 2000 ORION Workshop resulted in a rough facility outline with a few suggested parameters. But there were many options available that would require reduction to achieve a baseline design. This was the starting point for the present Technical Design Study (TDS). A review of the beam requirements for anticipated experiments was carried out for the TDS, and some representative results are summarized in Table 1. Both low energy (tens of MeV) and high energy (hundreds of MeV) beams are desired as well as a wide range of bunch charges (pC to nC) and normalized emittances (~10^{-6} to 10^{-5} m-rad, rms).

Table 1. Anticipated Experimental Beam Requirements

Experiment	**Bunch Structure**	**Energy (MeV)**	**Comments/Critical Parameters**
Plasma Wakefield Acceleration	Drive bunch, 1 nC Witness bunch, 0.1 to 0.2 nC	30 - 350	Drive bunch length ≤ 2 psec, rms Time interval between bunches adjustable over 0.1 to 1 psec
Plasma Focusing of Beams	Single bunch, Variable charge	50 - 350	Emittance ≈ 4 to 40×10^{-6} m, rms
Laser Acceleration (λ = 1.6 - 2.5 μm)	Single bunch, 2 - 20 pC	50 - 350	Emittance ≤ 10^{-5} m, rms Bunch length ≤ 2 psec, rms Energy spread ≤ 10^{-3}
Ion Channel Laser	Single bunch, 1 nC	50 - 350	Bunch length ≤ 2 psec, rms
Electron Beam Hose Instability	Single bunch, Variable charge	50	Bunch length ≈ 2 psec
Amplified Cherenkov Wakefield Acceleration	Drive bunch, 1 to 3 nC	350	Low-charge witness bunch follows at a variable time behind drive bunch
High Brightness Electron Sources and Emittance Compensation	Single bunch, 1 nC goal	20 - 350	Emittance ≤ 2×10^{-6} m, rms goal

ORION experiments need a high-brightness electron source capable of single or few-pulse operation. The Next Linear Collider (NLC) Project will also benefit from such a pulsed source for cavity-mode and amplitude-phase studies. A laser-driven, radio-frequency (RF) photoinjector is the conventional approach today for high-brightness electron beams. An X-band (11.4 GHz) photoinjector is natural for the NLCTA linac, but there is little experience with these devices at this frequency. No performance record exists for such a source, and its development introduces significant risk to the construction schedule. Several variations of the so-called BNL/SLAC/UCLA photoinjector at S-band (2.856 GHz) have been built which yield bunch populations and emittances similar to the requirements in Table 1. Based on this performance history, an S-band photoinjector design, optimized for minimum emittance at a bunch charge of 0.25 nC (1.5×10^9 electrons), and adjustable up to a nominal maximum of 1 nC, was chosen as the baseline for the TDS.

Maximizing the utility and flexibility of the facility for users while ensuring personnel safety will be designed into the ORION Facility from the start. The ORION safety interlock system will be integrated into the existing NLCTA interlock chain. The present concept is to design the system to permit access to an experimental hall when its two redundant, moveable beam stops are in place. This facilitates hall access by staff and users without interrupting NLCTA beam operations. Beam can only enter an experimental hall when the hall doors are shut, and the moveable beam stops are actively maintained in the open state. Since the laser rooms are outside the radiation areas and separately interlocked, access to them will be allowed when beam is enabled in the NLCTA and experimental halls. Finally, for laser set-up and calibration, it is necessary to have access to the NLCTA enclosure and experimental halls when a laser is operating provided that the appropriate personal protective equipment is in use.

2.3 ORION Facility Design

2.3.1 Machine Parameters

Beam physics analyses and initial engineering design, described in the body of this report, resulted in the general design parameters for the ORION Facility in Table 2. These values are compatible with the anticipated experimental needs of the initial science program. The choice of rf system was based on the availability of S-band klystrons and state-of-the-art, solid-state modulators at SLAC. The laser system described in the table is that for driving the photoinjector and will reside in Laser Room 1 (Fig. 1). Any special lasers for experiments are placed in Laser Room 2. The drive laser for the source will be configured to supply up to two bunches for pump-probe and wakefield experiments. The laser energy per pulse will be split to achieve this, and hence the sum of the bunch populations is not expected to exceed the maximum single-bunch population. Upgrades to more efficient cathodes, such as magnesium, or higher laser energies will be considered if experimental needs demand.

Table 2. General Design Parameters of the ORION Facility

Beam Energies	7 MeV (Source); 7-67 MeV (LE Hall); 67-350 MeV (HE Hall)
Charge per Bunch	0.25 nC optimum, adjustable up to a nominal maximum of 1 nC
Number of Bunches	1 or 2 (split charge)
Transverse Emittance	$\leq 2\times10^{-6}$ m , normalized rms (0.25 nC)
Bunch Length	1.8 psec, rms (0.25 nC)
Charge Stability	±2.5% pulse-to-pulse
Bunch Timing Jitter	0.25 picosec, rms
Repetition Rate	10 Hz
Average Beam Power	0.67 W at 67 MeV; 3.5 W at 350 MeV (1 nC bunches)
Electron Source	1.6 cell, S-band (2.856 GHz) Photoinjector
Drive Laser	Commercial Ti:Sapphire, 266 nm wavelength, 1 mJ output
Source RF System	SLAC 5045 Klystron; Solid-State, NLC-type Modulator
Injector Linac	Two X-band (11.4 GHz), 0.9 m, 30 MV, NLC structures
High-Energy Linac	Four X-band, 1.8 m, 72 MV, NLC structures

The electron-source beam energy is about 7 MeV, and the transfer line to the Low-Energy (LE) Hall is designed for beam energies from 7 MeV to 67 MeV, limited by the acceleration fields in the injector sections. The available rf power and the four NLCTA linac sections determine that the nominal beam energy supplied to the High-Energy (HE) Hall is 350 MeV. The transfer line to the HE Hall will be designed for beam energies from 67 to 1170 MeV, the upper design limit of the NLCTA radiation shielding. This permits the program to take advantage of future high-gradient, NLC accelerator sections. Experiments in the LE and HE halls may produce highly energetic particles downstream but at low average currents. Experimental hall shielding of the same thickness as the NLCTA enclosure is envisioned since the latter was conservatively designed for up to 5.5 nA average current loss of 1170 MeV electrons at any point.

2.3.2 Electron Source and Injector

A natural choice for the operating frequency of the ORION photoinjector is 11.424 GHz, due to the X-Band linac in the NLCTA. Although research is proceeding, no operational experience exists for photoinjectors at this high frequency. In order to eliminate as much photoinjector research and development from the ORION construction project as possible, a design based on the S-band Next Generation Photoinjector (NGP) (Ref. 6,7) was chosen. This design is employed at the majority of photoinjector labs now in existence, including the BNL Accelerator Test Facility, Neptune and PEGASUS at UCLA, and the Gun Test Facility at SSRL/SLAC. The NGP, which was developed originally as an ultra-low emittance injector for advanced light sources, is comprised of a modified version of the BNL/SLAC/UCLA 2.856 GHz, 1.6 cell rf gun along with a single emittance compensation solenoid magnet.

The optimum conditions for obtaining the best emittance performance out of this photoinjector, run at 140 MV/m peak field, while employing an S-band travelling wave section, has been studied numerically by the Linac Coherent Light Source (LCLS) collaboration (Ref. 8). The implementation of the RF photoinjector and linacs at the NLCTA can be made very similar to that of the LCLS design with the same linac gradient and external solenoid focusing. The accelerating gradient and solenoid strength in the LCLS design have been chosen to match the beam's space-charge dominated waist at the first linac entrance (150 cm from the photocathode) to the invariant envelope (Ref. 9), which is the optimum condition for the final compensation of the beam emittance. Certain beam parameters are sensitive to the change in rf environment when injecting a beam created by an S-band photoinjector into an X-band accelerator. The invariant envelope is dependent on beam current, accelerating gradient and external solenoid focusing. Since the last two of these can be made to approximate the LCLS injector case, the relative positions of the photocathode and first linac entrance will be kept at 1.5 m separation in the ORION design. On the other hand, X-band sections are much smaller in iris dimension, which means that beam scraping, energy spread, and wake effects are more severe in these linacs.

Beam dimensions in an emittance compensated photoinjector can be scaled with the beam charge as $\sigma \propto Q^{1/3}$ while maintaining optimized performance without altering the accelerator or beam optics settings (Ref. 10). This insight is critical to the injector mission, as the ORION program will demand both high charge beams for wakefield acceleration experiments, and very low charge, low emittance beams for direct laser acceleration experiments. The natural scaling with rf wavelength, $Q \propto \lambda_{RF}$, suggests that Q = 0.25 nC (reduced from 1 nC in the LCLS) is a reasonable choice for the reference design charge for ORION. As part of the design's refinement, the beam optics design will be tested computationally from 1 pC up to about 4 nC, which is considered the maximum range of charges needed by experimenters during the first years of operation.

The design of the ORION beamline with the rf photoinjector and X-band linacs is shown in Figure 2. In the NLCTA, the first two linacs are 0.9 m, X-band sections and are equipped with large external solenoids over their entire length. At a voltage of 30 MV per section, the average accelerating gradients are about the same as in the LCLS design (33 MV/m). The results quoted here are for a 60 MeV beam, but future calculations will include the entire 7 to 67 MeV range of the injector. It should be noted that the gradients, however, are not constant along each section, as the shunt impedance was designed to rise along the linacs to negate the effects of strong beam loading while the thermionic source was in use. Thus in single-bunch mode, the accelerating field increases along the sections. In addition, in order to capture the low-energy (100 keV) dc beam emitted by the thermionic source, two 6 cm long, prebuncher cavities are installed before the first traveling wave sections. These are neglected in the longitudinal beam optics design since at their low power levels they cannot significantly change the dynamics of the 7 MeV beam. The first prebuncher, 1.1 meters downstream from the photocathode, will be removed from the ORION beamline. The second is physically part of the first X-band section and will remain.

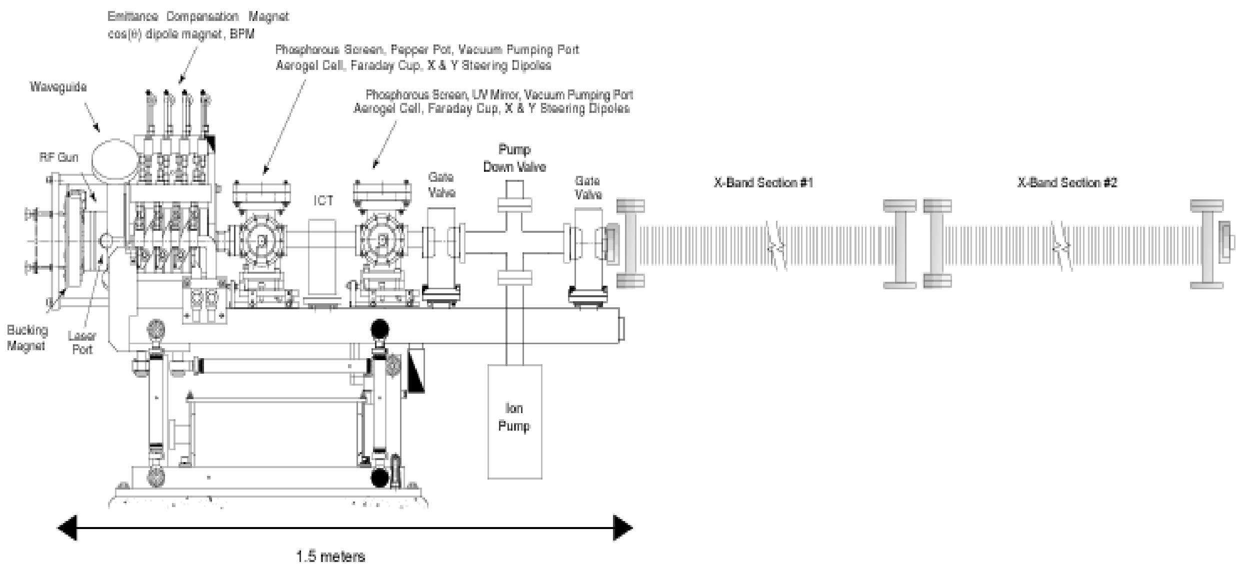

Figure 2. Schematic diagram of the complete ORION injector line with S-band photoinjector, emittance-compensation solenoid, diagnostics section, vacuum-box interconnect and the two NLCTA X-band linac sections.

The optics design for the ORION injector reference case has been preliminarily optimized by HOMDYN simulation. HOMDYN is a code which calculates the self-consistent linear optics of the photoelectron bunch by slicing it into many longitudinal slices, and allowing these slices' envelopes to evolve under their different rf phase and space-charge environments (Ref. 8). These simulations have been benchmarked against multi-particle codes such as PARMELA (Ref. 11), and have been shown to predict correctly the conditions where emittance compensation is obtained. The relevant parameters describing the conditions found in this optimization process are given in Table 3. The transverse and longitudinal electromagnetic fields in the 1.6 cell structure are those for a TM01,π-mode as calculated from SUPERFISH (Ref. 12) and described in Section 3.2. These simulation parameters produce a beam of over 60 MeV in final energy. The results of this simulation are summarized in Figures 3 and 4.

Table 3. HOMDYN Simulation Parameters for the ORION Injector Reference Design

Bunch charge	0.25 nC
Injected bunch length (flat-top)	6.3 psec
Injected beam radius (flat-top)	0.63 mm
Photoinjector accelerating gradient	140 MV/m
Peak gun solenoid magnetic field	3.09 kG
Launch phase (centroid)	33 degrees
Initial accelerating gradient in X-band linacs	33.6 MV/m
Solenoid field in X-band linacs	0.7 kG

In Figure 3, the transverse rms beam size and normalized emittance are given as a function of distance along the beam line. The simulated emittance compensation performance in the 0.25 nC reference case is impressive, with a final value after acceleration of $\varepsilon_{x,n}$ = 0.1 mm-mrad. As HOMDYN only includes the linear component of the emittance induced by space-charge and rf forces, nonlinear contributions to the emittance (Ref.13, 14) must be calculated using a particle code such as PARMELA. From previous experience, the emittance is typically larger in PARMELA by a factor of 2 to 3 as compared to the HOMDYN predictions. Experimental measurements of the transverse emittance in photoinjector beams have typically been a factor of 2 higher than that predicted by PARMELA. This may be due to the inaccurate modeling of the complicated 3-D electromagnetic fields in the cavities, image-charge effects at the cathode and inaccurate initial conditions for the beam launched from the cathode. To take into account such uncertainties, a conservative design emittance of $\leq 2\times10^{-6}$ m, normalized rms, at 0.25 nC has been adopted in Table 2. For different charges, the emittance scales theoretically as $\varepsilon \propto Q^{2/3}$.

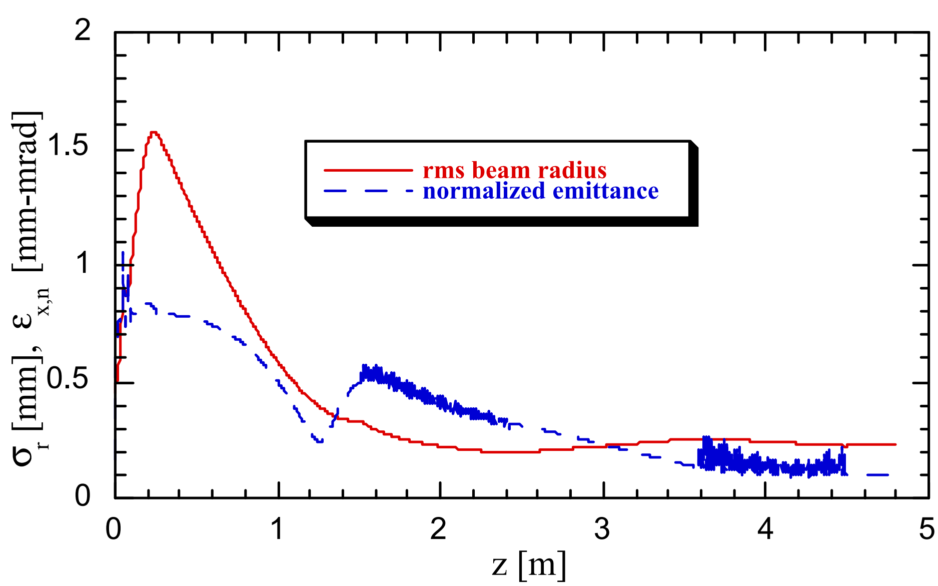

Figure 3. Evolution of the transverse rms beam size and normalized emittance of a 0.25 nC bunch as a function of distance along the injector axis for the ORION reference design case, from HOMDYN simulation. The first X-band section begins at 1.5 m and the second at 3.6 m.

From previous comparisons with PARMELA, the beam radius predicted by HOMDYN is expected to be reasonably accurate. This allows an evaluation of the maximum charge emitted from the S-band photoinjector and focused by the emittance compensation solenoid that will be within the aperture of the X-band structures. The iris of the prebuncher cavity connected to the X-band section sets the first aperture limit since the injected beam is widest there. The iris of this cavity is 7.5 mm in diameter. The 0.25 nC beam at the entrance to the buncher cavity (at 1.5 m in Figure 3) has an rms size of 0.35 mm. To adopt a conservative margin for avoiding beam halo scraping, the edge of the beam is taken to be roughly four times this value, or 1.4 mm radius. The full beam radius expands to 3.75 mm (iris radius) when the beam charge is scaled to 4.8 nC (from the one-third power law). Thus, charges up to about 5 nC can be injected. The aperture of the X-band accelerator sections is 8.1 mm diameter at the narrowest point (downstream end). The 0.25 nC beam has an rms size of 0.25 mm inside these sections. The full beam would expand to fill the accelerator aperture at 17 nC, so the charge limit is in fact set by the prebuncher aperture.

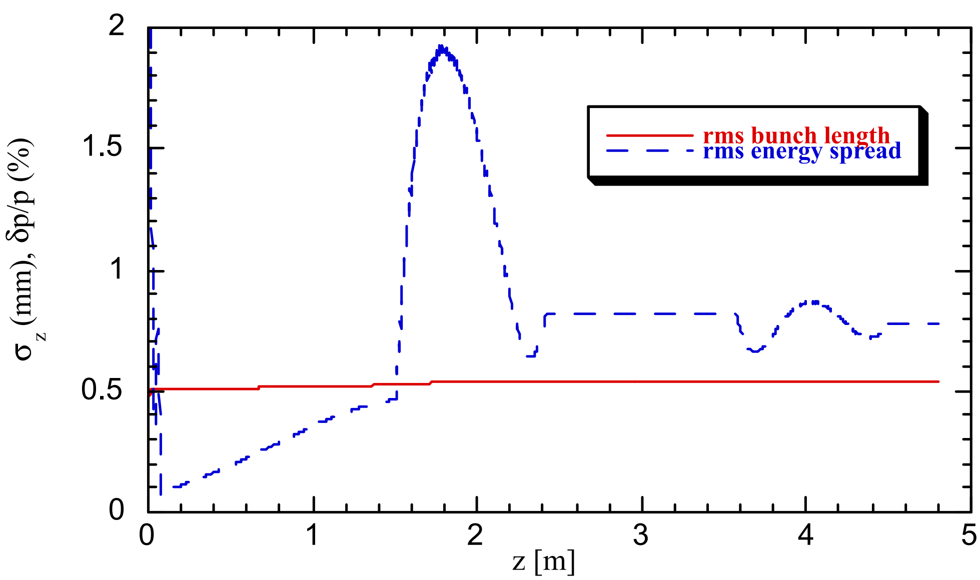

Figure 4. Evolution of the rms bunch length and relative energy spread of a 0.25 nC bunch as a function of distance along the injector axis for the ORION reference design case, from HOMDYN simulation. The first X-band section begins at 1.5 m and the second at 3.6 m.

In this design, the beam pulse length, illustrated in Figure 4, is well preserved from injection at 0.55 mm, rms or 1.8 psec $(\sigma_z = c\sigma_t)$. This corresponds to a phase spread of 7.5 degrees at X-band. Thus the total momentum spread for the reference design is not small, being limited to at least $\sigma_{\delta E/E} \cong \frac{1}{2}\sigma_\phi^2$=0.8%. For cases where smaller energy spread is required, shorter laser pulses (with concommitant lower charges) must be injected. Bunch length on the other hand is adjustable using the magnetic chicane, as described in Section 2.3.3.

2.3.3 Beam Manipulation, Extraction and Transfer

Beam must be extracted from the NLCTA linac to supply the Low and High-Energy Halls. A natural point to extract low-energy beam is after the magnetic dipole chicane (Figure 5). At the high-energy end, beam can be extracted after the spectrometer magnet via a hole bored through the terminating beam stop. A new terminating beam stop will be installed at the end of the High-Energy Hall. The original design for the injector, chicane and high-energy acceleration line are described in the NLCTA Conceptual Design Report (Ref. 3).

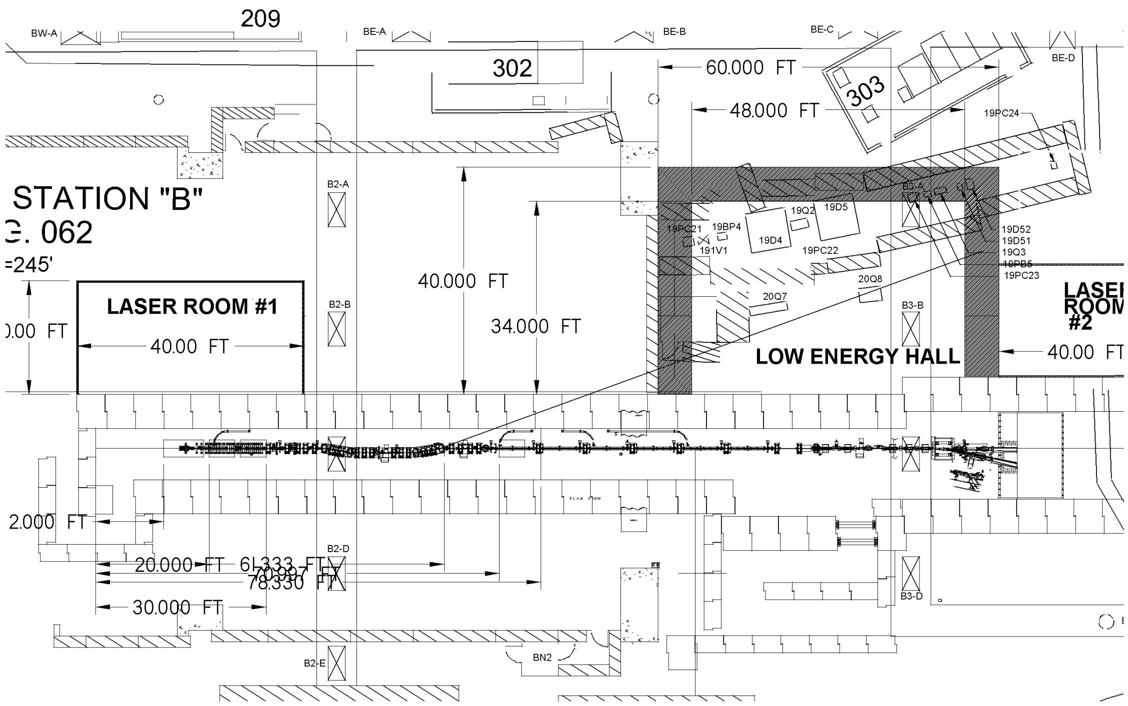

Figure 5. Detailed plan view of the ORION Facility at the NLCTA showing the transfer line to the Low-Energy Hall (center) and the NLCTA spectrometer and terminating steel/concrete beam stop, which will mark the entrance to the High-Energy Hall (right).

In order to minimize civil construction and disassembly of the NLCTA radiation shielding and waveguide plumbing, the proposed solution for transporting the low-energy electron beam to the Low-Energy (LE) Hall is through a beam pipe, 5 meters in length, set in a hole bored through the concrete shielding. The line will be at a 20-degree angle relative to the linac. A commercial version of TRANSPORT (Ref. 15) was utilized to model the low-energy transfer line, starting at the chicane entrance and proceeding through the five-meter beampipe. The Twiss parameters for the 0.25 nC, 60 MeV beam entering the chicane are α = -1.45, β = 1.75 m, and $\varepsilon_{x,n}$ = 0.45 mm-mrad, rms. Figure 6 is a preliminary simulation of the low-energy transfer line. Two quadrupole triplets powered in series and separated by a 5-meter drift were modeled. The maximum rms beam size reaches about 6.5 mm at the second quadrupole triplet. To have a 4-sigma safety factor to prevent beam-halo scraping, the beam pipe inner diameter must be 5 cm at this point. A 10 cm diameter hole bored through the concrete shielding is adequate to accommodate the beampipe and flanges.

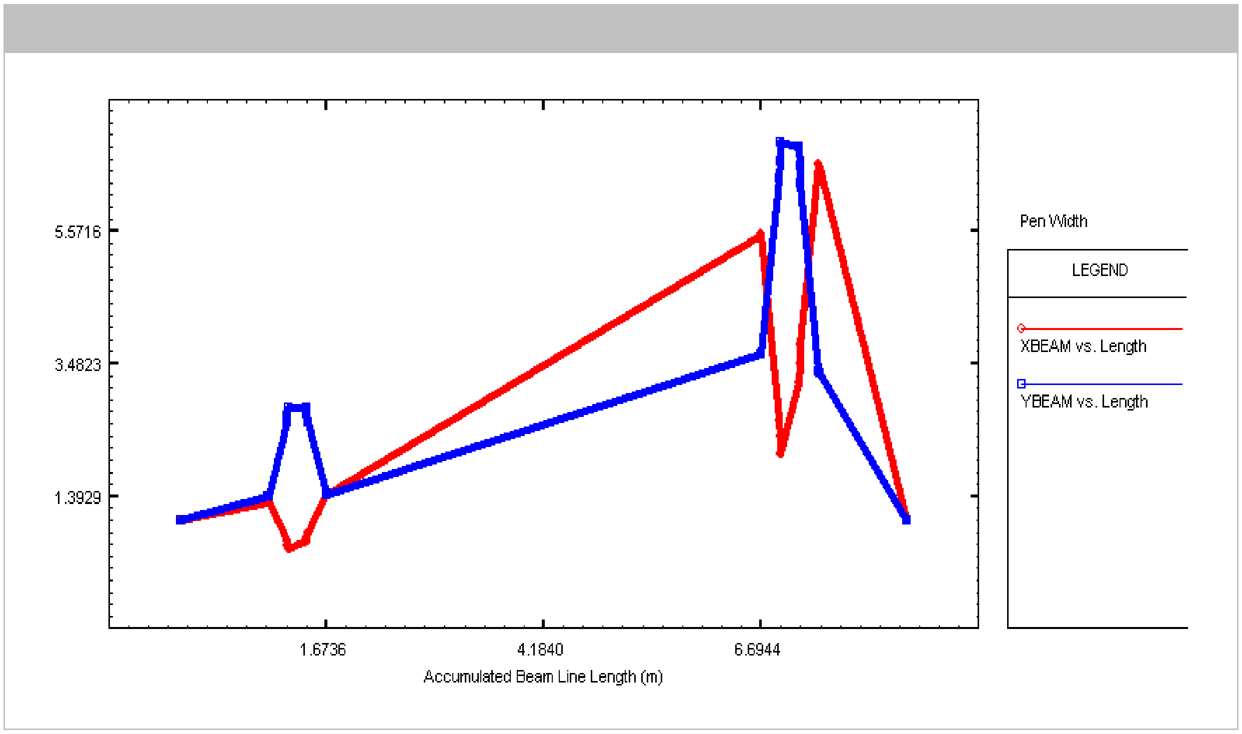

Figure 6. Evolution of the x (lower) and y (upper) rms beam sizes in millimeters as a function of distance along the transfer line to the Low-Energy Hall.

Extraction of the high-energy beam from the NLCTA for transfer to the ORION High-Energy (HE) Hall will occur downstream of the existing spectrometer magnet. Both a straight-ahead line and a 20-degree line exit from the magnet and presently terminate in a fixed, iron and concrete beam stop (Figure 5). Two holes will be bored through this beam stop. The present plan is to use the straight-ahead hole to transport beam for the initial high-energy ORION science program. The hole along the 20-degree angle will be plugged with steel shielding to maintain use of the spectrometer magnet. This hole will be available if needed to supply beam for a future upgrade of the HE Hall. A new spectrometer dipole magnet and a terminating beam stop identical to the present NLCTA stop will be installed at the end of the HE Hall.

The entry beamlines for both experimental halls will each have two redundant, moveable beam stops, which when closed, will allow personnel access to the halls even when beam is enabled in the NLCTA enclosure. Only when the hall access doors are interlocked shut and both beam stops are held open actively will beam be enabled to enter the hall.

Plasma and laser acceleration experiments at ORION will require a large range of bunch lengths and even tailored longitudinal bunch profiles. Bunch length compression using magnetic chicanes (four dipole magnets arranged in alternating polarity pairs to create two opposite orbit bumps) is now a standard technique in many rf photoinjector labs around the world with achieved pulse lengths measured well below the picosecond level. Correlated momentum variation in a bunch implies corresponding path length differences in a magnetic transport line, resulting in correlated arrival times, and hence bunch length, downstream. The ORION Facility will take advantage of the existing NLCTA chicane (Fig. 7) and further develop this technique to create pulses which are not only short, but have optimized profiles, and ultra-short trailing pulses.

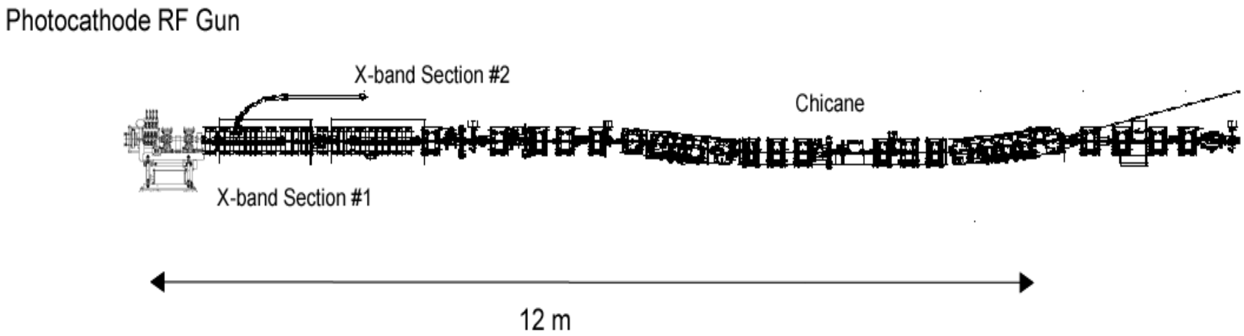

Figure 7. Layout of the ORION injector, with S-band rf gun preceding two X-band linacs, followed by NLCTA low-energy optics and chicane. The total length to the end of the chicane is 12 m.

Recent work at UCLA has shown that if instead of using a chicane-like transformation to remove the momentum-chirp imparted by running the linac off the wave crest, one uses a negative R_{56} transport line (Ref. 16), then a ramped pulse can be obtained, as shown in Figures 8 and 9. In this case, because $R_{56} \equiv \partial z_f / \partial(\delta p / p)_i < 0$, the beam is behind the rf wave crest, and effects such as wake-fields and longitudinal space-charge aid the compression process, making it even more powerful. The phase space associated with this process displayed in Fig. 8 creates a projected current distribution with a ramped rise and a very sharp fall, that is nearly ideal for driving wake-fields with a high transformer ratio (ratio of acceleration provided after the bunch to deceleration inside of the bunch). This current distribution, along with the theoretically predicted optimum pulse shape (Ref. 17, 18), and simulated plasma wake-fields driven in a $n_o = 2 \times 10^{16}\ \mathrm{cm}^{-3}$ plasma, are shown in Fig. 9. The chicane in the NLCTA beamline is nominally tuned for R_{56}=0, and thus both negative and positive values of R_{56} may be utilized, as experiments require. This type of pulse shaping is unique to the ORION program because the existing chicane and (naturally negative R_{56} transport to the experimental halls) allows fine tuning of this type of compression.

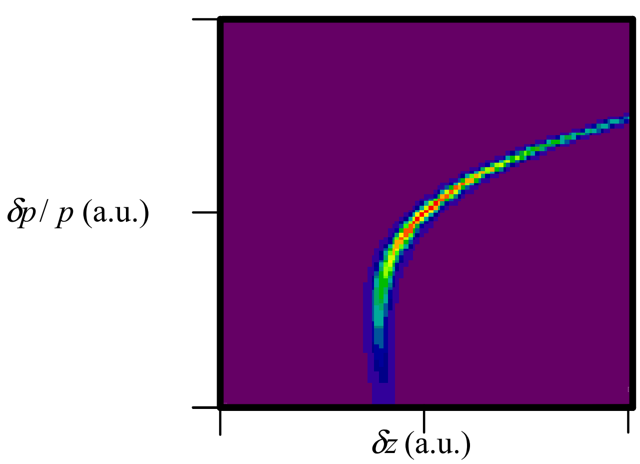

Figure 8. False-color plot of the simulated longitudinal phase space after compression using a negative R_{56} magnetic chicane system at ORION to obtain the ramped beam profile seen in Fig. 9.

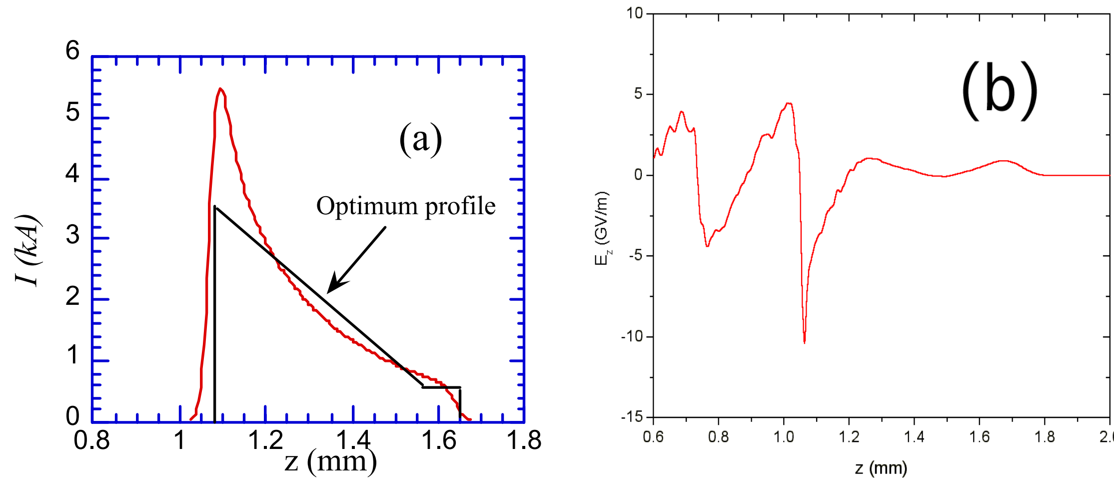

Figure 9. (a) Current profile of 4 nC beam phase space shown in Fig. 8, with optimal theoretical profile for driving a plasma wake; (b) PIC simulated wake-fields generated by the beam in a $n_o = 2\times 10^{16}$ cm^{-3} plasma.

Creation of such a tailored electron beam pulse is representative of the central mission for ORION, which is to provide enabling techniques in advanced accelerator experiments. Another related topic would be the generation of a slightly delayed "witness" pulse for probing the accelerating wake-fields downstream of the drive beam. While this has been accomplished in a single photoinjector, and the pulse propagated through a chicane compressor in the UCLA/ANL/FNAL plasma wake-field acceleration (PWFA) experiments (Ref. 19), it has not been envisioned for a negative R_{56} compression line. This situation presents particular difficulties, since when the compression is optimum, no particles exist behind the falling edge of the current profile (see Figs. 8 and 9). By further under-compressing (~2% smaller R_{56}), a larger trailing tail in the current profile can be created. If a collimator is then introduced at a high dispersion point in the compressor line to "notch" the momentum distribution, the end of the trailing tail can be separated from the majority of the drive beam, as illustrated in Fig. 10. This will allow introduction of a witness beam into the stable (phase focusing) region of the plasma wave excited by the drive beam (Fig. 9b).

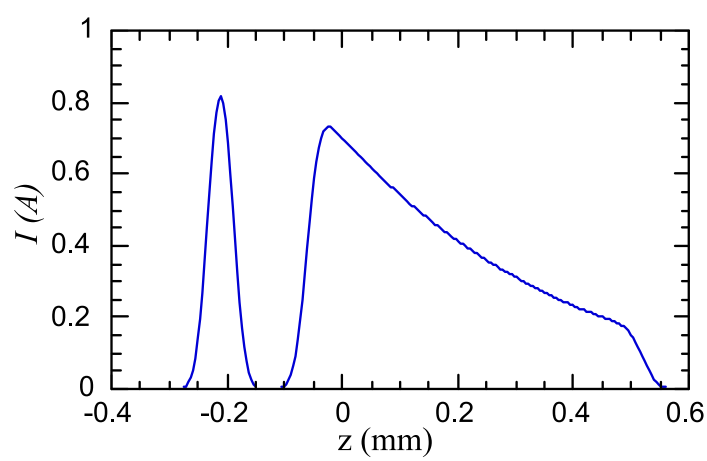

Figure 10. Current profile for a 4 nC beam with compressor further detuned, and momentum notch collimator used to produce a witness beam.

WORK IN PROGRESS:
DESCRIPTION OF THE BEAM DYNAMICS CALCULATIONS FOR HIGH ENERGY BEAM EXTRACTION AND TRANSPORT TO HE HALL.

2.3.4 End-to-End Simulations

WORK IN PROGRESS:
COMPLETE BEAM SIMULATION FROM THE SOURCE TO THE LOW-ENERGY AND HIGH-ENERGY HALLS.

2.3.5 Radiation Shielding

The NLCTA injector with its thermionic source was designed to be capable of producing a multi-bunch beam exiting the chicane with 7×10^{11} electrons per pulse at a repetition rate of 10 Hz (1.1 micro-ampere average current). The present NLCTA shielding design is conservative allowing for up to 0.5 percent of an 1170-MeV beam (6.6 W), or up to 9 percent of a 630-MeV beam (62 W) to be lost in the beam line at one point for 1000 hours per year. The terminating beam stop is designed to absorb the full 1170-MeV beam at 1.1 micro-amp average current (1300 W) and maintain an exterior dose equivalent of less than 1 mrem per hour.

Operating at 10 Hz and the highest anticipated bunch charge of 4 nC, the ORION photoinjector would produce up to 40 nano-ampere of average current. This is a factor of 25 lower current than the present NLCTA using the thermionic source under normal conditions. The Low and High-Energy Halls will be constructed with shielding equivalent to the NLCTA enclosure. Acceleration experiments in the halls can potentially produce very high-energy beams, but they will employ the photoinjector and not the thermionic source. Acceleration experiments will be limited to low repetition rates and low accelerated-bunch charges during start-up and be routinely monitored to characterize their radiation production. Each experimental beam line will be terminated with a beam stop capable of absorbing the maximum NLCTA beam of 1.1 micro-ampere at 100 MeV or 1170 MeV for the respective halls.

WORK IN PROGRESS:
DESCRIPTION OF THE PHOTOINJECTOR "SUPERCHARGED MODE" (BREAKDOWN) AND THE RADIATION ESTIMATE FOR THIS CASE.

3 Facility Components

3.1 Overview

The ORION Facility will be constructed in the environs of SLAC End Station B (ESB) at the existing NLCTA. A plan view of the facility is shown in Figure 1. The layout of technical components will be shown in detail in a SLAC Drawing, "ORION Technical Installation Master Layout", to be produced prior to construction start. The key modifications to the NLCTA are the ORION photoinjector with its S-band rf system, UV laser, and laser room, a 1600 square-foot, low-energy experimental hall (north side), an 800 square-foot laser room for user's and a 1000 square-foot, high-energy experimental hall (east side; upgradeable to 5000 square feet in the future if necessary). The present concept also includes the establishment of an approximately 3500 square-foot Staging Area in the planned SLAC Research Support Building, just northeast of ESB. Laser rooms and experimental halls will be interlocked, and the latter will have redundant, movable beam stops at the beam entrance and fixed, terminating beam stops at the end of experimental lines. Adequate water and power utilities already exist at ESB for ORION and only new distribution from electrical breakers and water mains is required. In the following sections, we describe the various technical components of the ORION Facility. Estimated costs for all items are in Section 5.3.

3.2 RF Photoinjector

The electrical and mechanical fabrication techniques for the S-band BNL/SLAC/UCLA rf photoinjector are well understood today given that several such devices have been constructed. The S-band photoinjector operates in the TM01,π-mode and is tuned to be resonant with the 2.856 GHz rf system. The cathode lies in the plane terminating the 0.6 cell, and the beam exits the photoinjector from the full cell (Fig. 11). This geometry places the cathode surface, and hence the electron bunch launched, in a high-field region (140 MV/m) in order to accelerate the electrons and rapidly reduce the deleterious space-charge forces. The 0.6 cell length introduces a third harmonic content to the cavity fields, which flattens the longitudinal electric field, reduces the cathode to iris field ratio and provides more rf focusing in the low-energy region. The 1.6 cell length is about 8.5 cm, making the structure's π-mode phase velocity synchronous with a particle near the speed of light.

The computer code SUPERFISH (Ref. 12) was used to determine the electromagnetic field properties of this structure, adjust the mechanical dimensions and derive frequency scaling laws for the cavity machining. At the 140 MV/m axial accelerating field determined by the beam optics design, the photoinjector requires about 15 MW of peak power. Operating at the 10 Hz repetition rate and a 3 μsec rf pulse length, the average power dissipation is 450 W. Frequency stability requires a temperature regulated water cooling system to maintain the cavity temperature to within $\pm$0.1 C of nominal. Waveguide coupling from the klystron source is through the outer wall of the photoinjector's full cell. To remove the field asymmetry induced by this coupling port, a vacuum port is placed on the opposite side. Two tuners are placed orthogonal to these ports, and the entrance and exit ports for the laser are located halfway between the tuner and rf/vacuum planes (Fig. 12).

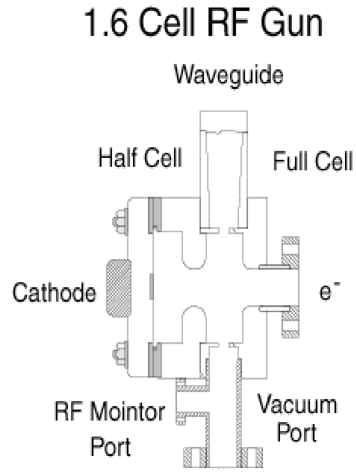

Figure 11. Cross sectional view of the 1.6 cell, S-band photoinjector.

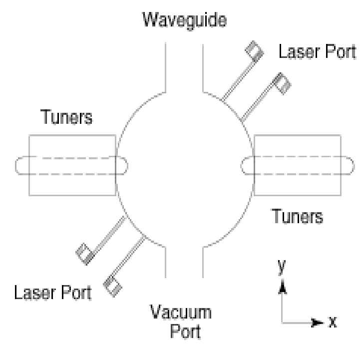

Figure 12. Arrangement of transverse penetrations into the 1.6 cell, S-band photoinjector.

The ORION source is a modified version of the prototype 1.6 cell photoinjector that is presently installed at the BNL Accelerator Test Facility. The ORION version has eliminated the use of the helico-flex as a combined vacuum and rf seal. The cathode/half cell vacuum joint of the ATF injector has been replaced with a 6 inch OD, rotatable stainless steel conflat knife-edge flange. Continuity of the rf current paths on the other hand is satisfied using press fit point-to-point contact between the half cell OD surface and the cathode plate edge. The edge of the cathode plate is Ti:N coated to facilitate cathode plate removal after high-temperature bake-out.

This arrangement allows for cathode inserts made of different materials to be retrofitted to the plate. Present photoinjectors use either metal cathodes such as copper and magnesium, or semiconducting materials such as cesium–telluride and gallium arsenide. Choosing an appropriate material is complicated by the fact that the environment under which the cathode operates involves ultra-high vacuum (10^{-9} Torr) and 100 MV/m fields. Cathode choice is a compromise between high quantum efficiency (electrons per photon), long lifetime, modest vacuum requirements, ease of material and surface preparation, work function comparable with available laser energies, and compatibility with high electric fields. A copper cathode was chosen for the baseline design because it is mechanically robust, simple to prepare, and in spite of its low quantum efficiency, bunch populations of 0.25 to 1 nC are achievable using commercially available 1 mJ UV lasers (Section 3.3). Table 4 summarizes the design parameters for the ORION photoinjector.

Table 4. RF Photoinjecter Parameters

Frequency	2.856 GHz
Acceleration Gradient	140 MV/m
Cavities	1.6 cells
Structure Fill Time	0.7 μsec
Cathode	Copper
Expected Quantum Efficiency	5×10^{-5}
Design Bunch Charge	0.25 nC, optimum
Charge Stability	± 2.5%, pulse-to-pulse
Beam Output Energy	7 MeV
Energy Spread	0.8%, rms
Nominal Bunch Length	1.8 psec, rms
Bunch Timing Jitter	0.25 psec, rms
Normalized Emittance	$\leq2\times10^{-6}$ m, rms
RF Input Peak Power	15 MW
RF Repetition Rate	10 Hz
RF Pulse Length	3 μsec
Average Dissipated Power	450 W

The 1.6-cell body is composed of OFE II (oxygen-free, high-conductivity, grade II) copper. Internal dimensions are machined to enforce field balance at the π-mode (i.e, the ratio of the peak accelerating field in the full-cell is equal to the cathode field in the half-cell). After final tuning of the full cell, the first hydrogen-braze step joins the full and half cells using 35%-65% gold-copper alloy (1025 C). After this braze, a cut-and-measure technique is used for the final half-cell tuning. Once the rf coupling, balanced field and π-mode tuning to 2.856 GHz is achieved, the second and final braze with 50%-50% gold-copper alloy (982 C) is performed.

The other essential element of the rf photoinjector is the emittance-compensation, solenoid magnet. The axial magnetic field and effective magnetic length needed to minimize the transverse emittance at the design charge come from the beam optics design described in Section 2.3.2. The computer code POISSON (Ref. 12) is used to design the solenoid. The electrical and mechanical parameters of the solenoid are given in Table 5.

Table 5. Solenoid Parameters

Nominal Axial Field	3 kG
Magnetic Material	1006 Steel
Conductor	Copper, hollow
Cross Section	0.395 cm^2
Resistance	0.086 Ω
Voltage	18.95 V
Power	3445 W
Current	220 A
Current Density	557A/cm^2

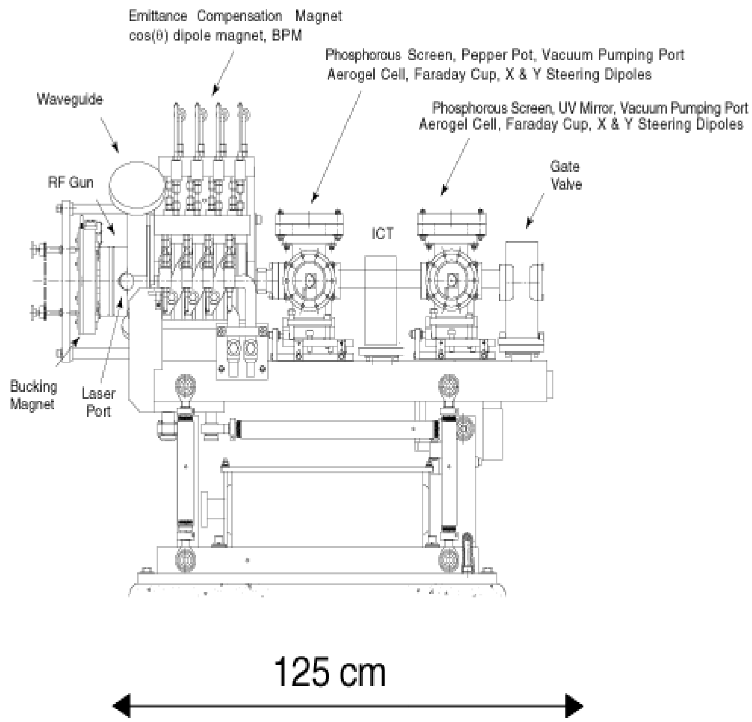

Figure 13. Schematic diagram of the ORION S-band, 1.6 cell photoinjector with emittance-compensation solenoid and diagnostics section.

A diagnostics section for measuring the beam exiting the photoinjector follows the solenoid and is mounted to the photoinjector girder. Figure 13 is a complete diagram of the photoinjector, solenoid and diagnostics section. A single diagnostic must span many orders of magnitude in dynamic range to be useful to operators of the ORION injector. The electron beam charge is expected to vary from 2 pC to 4 nC, and the bunch length from 150 fsec to 10 psec. The beamline distance of 150 cm from the cathode plate to the middle of the input coupler of the first of two X-band, 0.9 meter accelerating structures is determined by beam dynamics considerations (Sec. 2.3.2). In this limited space the rf gun, emittance compensation magnet, and low-energy photoinjector diagnostics must be placed. The injector region of the ORION Facility is shown in Figure 2. The suite of diagnostics must measure on a single-pulse basis the electron beam's charge, energy, spot size, bunch length, position, and emittance. Also beam steering and vacuum pumping must be accomplished here. To fully utilize the limited space, all vacuum joints in the injector rf gun region will consist of a rotatable-non-rotatable, UHV knife-edge joint pair with one of the flanges having tapped bolt holes. This will eliminate the need for the addition of space during the nut/bolt installation and tightening process.

The bore of the emittance compensation magnet houses three components: 1) the solenoid magnet, 2) cos(θ) dipole steering magnets and 3) a Beam Position Monitor (BPM). Using the cos(θ) dipole steering magnet and a down stream profile screen, the electron beam energy will be measured directly out of the photoinjector, but prior to the X-band accelerating section.

Immediately after the emittance compensation magnet, a single arm of a non-magnetic, stainless steel, six-way port will be utilized as a multifunction assembly with phosphorus screen, aerogel cell, pepper pot emittance measuring device and Faraday cup for charge measurement. In addition, a second arm will be used for an ion pump/vacuum assembly. A pair of X & Y dipole steering magnets will also be located here. All profile screens will have a set of fiducial marks in the field of view of its CCD (charge coupled device) camera. This will permit self-calibration during normal operation. Each CCD camera will have a remotely controlled light-source for illumination during alignment and calibration. In addition all CCD cameras used for injector alignment and calibration will be slaved to a master control system capable of recording and redirecting input data to various monitors located throughout the ORION Facility on demand.

A second six-way port will also be utilized as both a diagnostics and vacuum port. An arm of the second diagnostics six-way port contains a phosphorus screen, aerogel cell and Faraday cup. In combination with the pepper-pot of the first six-way port, the aerogel cell of the second six-way port, light-transport system and the Hamamatsu streak camera, the ORION Facility will have a state-of-the-art slice emittance measurement diagnostic. An optical transport system will send light from the injector diagnostics region to Laser Room 1B for analysis. In addition, a third arm of the second diagnostics port will be allocated to a nearly normal incident UV laser transport mirror. This mode of laser transport is not anticipated for initial operation of the ORION photoinjector, but it is included in the design to facilitate different laser transport schemes in the future. A third pair of X&Y dipole steering magnets will provide final steering into the 0.75 cm aperture of the X-band accelerating sections.

Located in between the two diagnostic six-way ports described above is a ceramic break for a gap monitor and an integrating current transformer (ICT). The two Faraday cups and the single ICT allows for redundant charge measurements in the drift space between the rf gun and the first of the two 0.9 meter X-band sections. Just before the entrance of the 0.9 meter, X-band accelerating sections, a UHV gate valve and vacuum transfer box allow for a relatively simple and fast disconnect of the RF photoinjector for occasional maintenance. By bringing up to air only a small section of drift space, this scheme will prevent exposing the ORION electron source or X-band linacs to any significant amount of gas.

3.3 Drive Laser System

The drive laser supplies the photons that are absorbed by electrons in the photoinjector cathode, allowing these to escape the surface if their kinetic energy exceeds the material's work function. The energy per laser pulse U(J) needed to produce a bunch of charge q(C) using photons of energy E(eV) (≥ work function) incident on a cathode surface with quantum efficiency QE (electrons emitted per incident photon) is given by U(J) = q(C)E(eV)/QE. A cathode's QE depends on many conditions, and variations by a factor of two are common (Ref. 20). Assuming a typical QE = 5×10^{-5} for copper (Ref. 6,7) and 5 eV incident photons, 10^{-4} J is required to produce a 1 nC bunch. Laser light will be absorbed by the various optical elements needed for pulse shaping as well as the elements needed for light transport to the photocathode. An estimated light-loss budget is needed to specify the laser energy.

Based on experience with other ultraviolet drive lasers (Ref. 6,7), a preliminary layout of the ORION laser system and transport line to the photocathode was made to derive an estimated light-loss budget. The laser transport layout is shown in Figure 14 and is based on a frequency-tripled IR to UV system. The light-loss estimate for this layout is given in Table 6. The first two entries give the maximum losses due to IR pulse masking prior to entering the harmonic converter. All entries following the converter refer to transport of the UV light to the photocathode. Multiplying all the efficiencies in the last column of Table 6 yields an overall efficiency of IR to UV delivered to the cathode of 0.078.

Table 6. Estimated Light-Loss Budget for the ORION Drive Laser System

Element	Loss per Element	Quantity	Total Efficiency
Fourier LCD Mask (IR)	0.10	1	0.90
Spatial LCD Mask (IR)	0.10	1	0.90
Harmonic Converter (IR to UV)	0.90	1	0.10
Grating	0.25	1	0.75
Cylindrical Lens	0.10	1	0.90
Mirror	0.02	15	0.74
Aperture	0.65	1	0.35
Polarizer	0.05	1	0.95
Lens	0.02	15	0.74
UHV Optical Port	0.08	3	0.78

A commercial Titanium-Sapphire (Ti:Sapphire) laser system adequate to produce bunch charges of 0.25 to 1 nC is described here, and its parameters are given in Table 7. A block diagram of the conceptual laser system is presented in Fig. 15. A diode-pumped, green laser pumps a Ti:Sapphire oscillator delivering 2 psec pulses at 80 MHz with a wavelength selectable from 720 to 850 nm (IR). An Nd:YAG pumped Ti:Sapphire regenerative amplifier produces ten individual pulses per second over a wavelength range of 750 to 840 nm and up to a micropulse energy of 10 mJ. After any spatial and Fourier masking for pulse shaping, these pulses are frequency-tripled in a series of nonlinear crystals to a nominal wavelength of 266 nm (UV). Depending on the amount of IR masking, the UV energy per pulse arriving at the photocathode is expected to be in the range 0.07 to 0.1 mJ. For the assumed QE, this is three to four times the energy needed for the nominal 0.25 nC charge. Bunch charges approaching 1 nC are feasible, and the system will be designed to allow a straightforward upgrade in the IR energy if necessary.

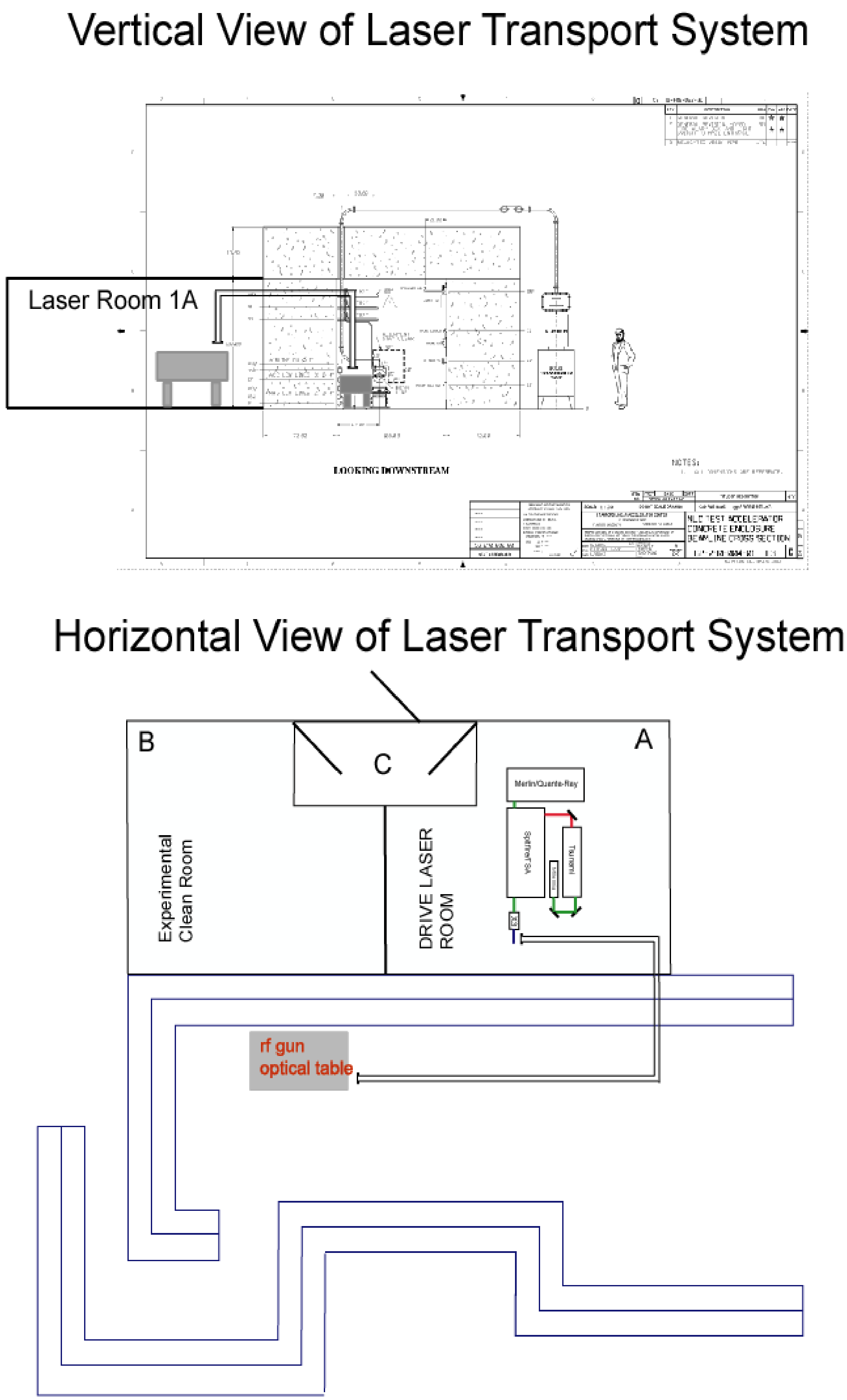

Figure 14. Layout of the drive laser transport system for the ORION photoinjector.

Table 7. Drive Laser System Parameters

Laser Type	Ti:Sapphire
Output Wavelength	266 nm
IR Energy ($\lambda \approx 800$ nm)	10 mJ (no masking)
UV Output Energy	1 mJ
UV Amplitude Jitter	± 2.5%, pulse-to-pulse
Pulse Number	1 or 2 (split energy)
Nominal Pulse Length	6.3 psec (flat-top)
Timing Jitter	0.25 psec, rms
Macro-pulse Rep. Rate	10 Hz
Cathode Spot Diameter	0.63 mm (flat-top)
Laser Incidence on Cathode	72 deg. from normal

To minimize the energy spread of the electron beam, the laser pulse length should be short compared to the rf wavelength, or less than 2.5 psec, rms (10 degrees at 11.4 GHz). A pulse stretcher/compressor consisting of a pair of matched gratings allows for control of the nominally 6.3 psec pulse length (flat-top) for optimization of the electron bunch characteristics. Laser pulse length will be adjustable over a range of 150 fsec to 10 psec to accommodate different experimental requirements. To satisfy the timing jitter for electron bunch arrival at the X-band accelerator of 0.25 psec, the laser pulse must arrive at the cathode at a consistent phase relative to the rf accelerating field. The laser system is mode-locked to a harmonic of the photoinjector rf system and stabilized to deliver the laser pulse to within 0.25 psec, rms, or one degree of rf phase at 11.4 GHz, for consistent bunch arrival timing. The laser amplitude in the UV must be stable to ± 2.5%, pulse-to-pulse, in order to maintain the corresponding bunch charge stability from the photoinjector. In a frequency-tripled system, the IR amplitude stability must be one-third of this value or ± 0.8%, pulse-to-pulse.

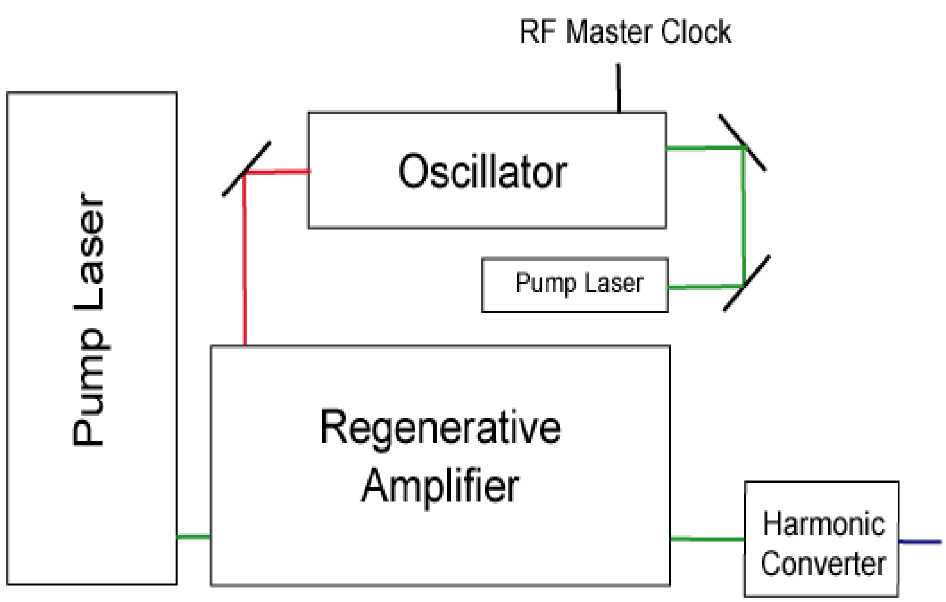

Figure 15. Block diagram of drive laser system for the ORION photoinjector.

3.4 Radio Frequency System

The 2.856 GHz, photoinjector requires a single, high-power S-band klystron and modulator system to power its accelerator cells. The 1.6 cells accelerate the electron bunch created at the cathode by the laser. To operate at the accelerating gradient of 140 MV/m, the photoinjector requires about 15 MW of peak rf power. The standard and proven SLAC 5045 klystron is immediately available on site and is the baseline choice. Its 65 MW output capability is more than adequate, and reliable operation is expected. The modulator choice is equally straightforward. A new solid-state modulator, consisting of twenty insulated-gate bipolar transistor (IGBT) drivers arranged in a pulse-forming network, has been designed at SLAC for the Next Linear Collider project (Ref. 21). A prototype has been successfully tested at full power with a SLAC 5045 klystron. Table 8 summarizes the RF System parameters. For completeness, the parameters for the downstream NLCTA rf system are included here (Ref. 22).

Table 8. Radio Frequency System Parameters

Accelerator Unit	ORION Source	NLCTA Sections
Radio Frequency	2.856 GHz	11.424 GHz
Klystron Type	SLAC 5045	NLC-XL4
Peak Power	65 MW	50 MW
Repetition Rate (for ORION)	10 Hz	10 Hz
Pulse Length (flat-top)	3 μsec	1.5 μsec
Perveance	2×10^{-6} A/V$^{3/2}$	1.2×10^{-6} A/V$^{3/2}$
Voltage	340 kV	400 kV
Current	396 A	300 A
Efficiency	0.47	0.42
Modulator Type	Solid State/NLC	PFN/NLCTA
Peak Power	138 MW	238 MW (2 klystrons)
Max. Repetition Rate	120 Hz	180 Hz
Voltage	23 kV	38 kV
Current	6 kA	12.5 kA
Pulse Transformer Ratio	15:1	21:1
Net Modulator Efficiency	0.80	0.73
Charging Supply Power	62 kW (120 Hz)	88 kW (180 Hz)

With the nominal 47 percent efficiency of the S-band klystron at 65 MW, the modulator is specified for 138 MW peak power. The modulator output pulse at 23 kV and 6 kA is transferred to the klystron through a 15:1 pulse transformer to produce the required 340 kV, 396 A for the klystron (Figure 16). The modulator efficiency is 80 percent and a single charging supply, rated at an average power of 62 kW (120 Hz), feeds the twenty IGBT parallel drivers. The ORION photo-injector is specified to operate up to a 10 Hz maximum rate. The modulator will be limited to this rate but operated at the full 138 MW level for NLC reliability testing. The rf power from the klystron will be split with 15 MW going to the photoinjector and the excess power available for an rf test station (or discarded into a water load when not in use).

The rf power will be transferred to the photoinjector through an evacuated waveguide and pass through a circulator (for klystron protection from reversed power flow) prior to entering the NLCTA enclosure. Sulfur-hexafloride (SF-6) gas at 24 psi is used in the circulator to reduce electrical breakdown problems. The required field amplitude stability in the photoinjector is 1 percent. If the downstream linac were S-band, the phase stability would be the usual 1 degree or 1 psec (0.3 mm) at 2.856 GHz. But the photoinjector beam is transferred into an X-band accelerator, so the phase stability is actually 1 degree at 11.4 GHz, or 0.25 psec (0.075 mm).

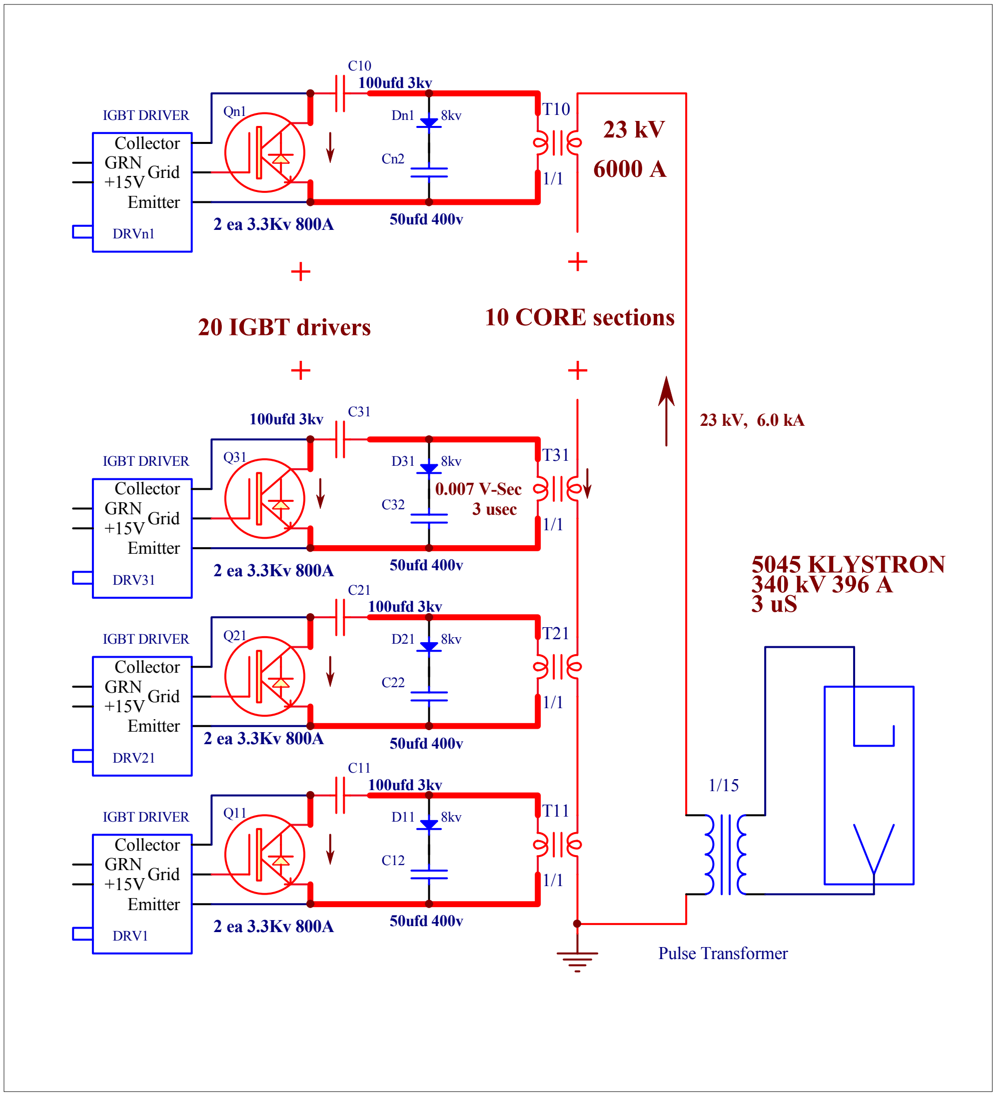

Figure 16. Block diagram of the S-band rf power system for the ORION photoinjector.

3.5 Transfer Lines

Extraction of beam for the Low-Energy Hall (7 to 67 MeV) occurs immediately after the chicane section of the NLCTA injector. The beam must be transported through the north shield wall. The shielding blocks for the walls and roof of the NLCTA enclosure are of a staggered-joint design for earthquake stability and radiation containment. With the substantial rf waveguide on the roof, disassembly of these blocks would be very difficult and expensive. Instead, a five-meter long, ten-centimeter diameter hole will be bored at a roughly 20-degree angle through the NLCTA shielding wall. Quadrupole magnet triplets will be used on either side of the wall to transport the beam (Figure 17). Shielding blocks of thickness equivalent to the existing wall will surround the new beamline. Note that the separation between adjacent beamline centers in the Low-Energy Hall is about 8 feet to facilitate experimental installation and maintenance.

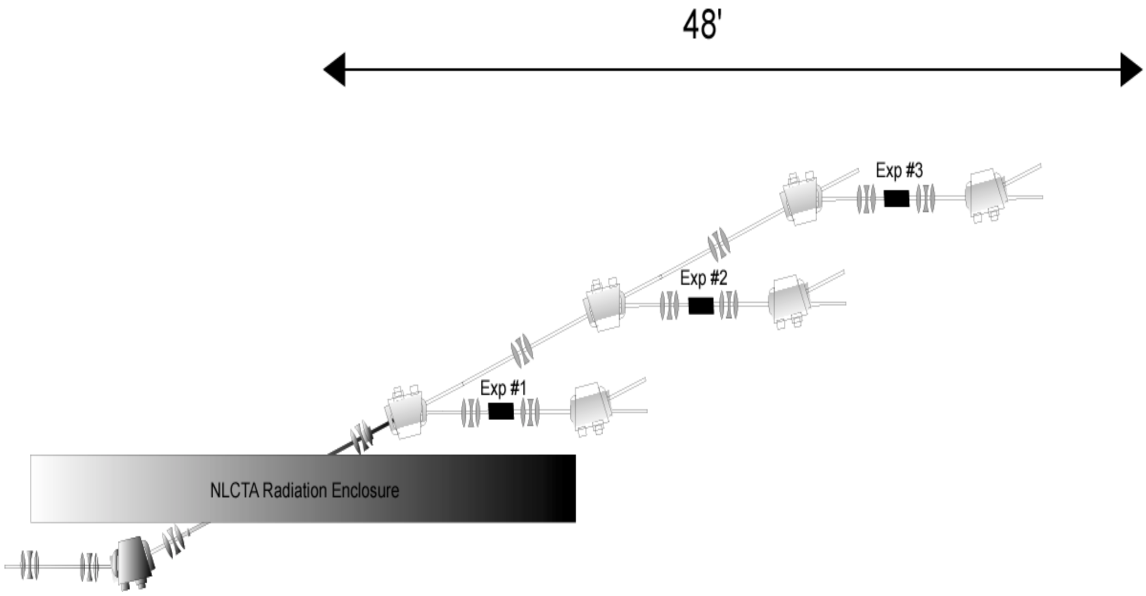

Figure 17. Conceptual drawing of the Low-Energy Transfer Line and beam lines in the Low-Energy Experimental Hall.

Extraction of beam for the High-Energy Hall (67 to 427 MeV) is done through the NLCTA spectrometer magnet (Figure 18). The NLCTA terminating beam stop will remain in place and two beam holes will be bored through it during the ORION civil construction. The angled hole will be plugged with steel so the spectrometer remains usable, but this hole will be available in the future if such a beamline is ever needed. Beam for the HE Hall passes straight ahead, and a new terminating beam stop will be installed at the end of the HE beamline. The present plan is to have two redundant, moveable beam stops at the beamline entry points to each hall so personnel can conduct installation and maintenance of experiments even when beam is present in the NLCTA enclosure.

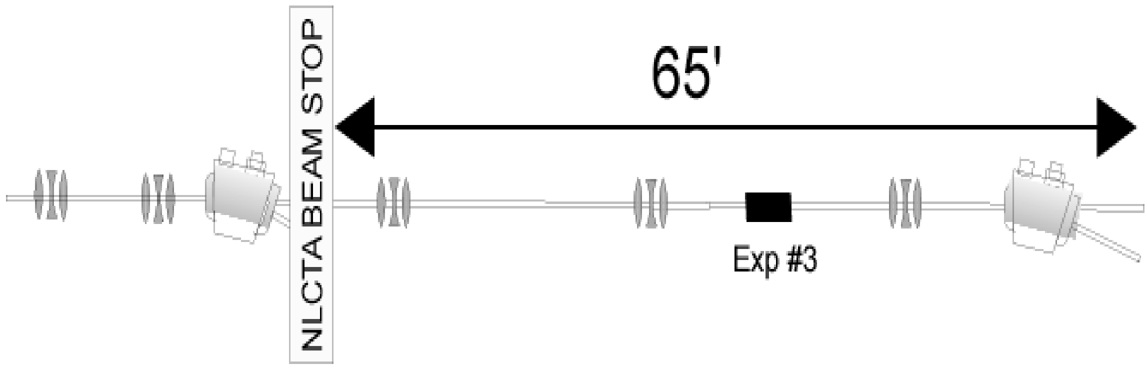

Figure 18. Conceptual drawing of the transfer line to the High-Energy Experimental Hall.

The ORION beamlines will require several new magnetic elements for beam transport. Table 9 lists the presently installed NLCTA magnets and the anticipated magnets for ORION by section, as designated in Figure 19. It is presently envisioned that the magnets in the LE and HE Hall beamlines will be fabricated and installed once the ORION operational phase begins.

Table 9. Presently Installed and [Anticipated] Magnets for ORION by Beamline Section.

	Source to Injector	**Injector to LE Hall Line**	**Low-Energy Hall Beamlines**	**LE Hall Line to HE Hall**	**High-Energy Hall Beamline**
Figure 19 Location	**A**	**B**	**C**	**D**	**E**
BEAM ENERGY	7 MeV	7-67 MeV	7-67 MeV	67-350 MeV	67-350 MeV
Quad Triplets					
QE	0/[0]	17/[17]	0/[0]	11/[11]	0/[0]
QF	0/[0]	0/[0]	0/[0]	5/[5]	0/[0]
NLC	0/[0]	0/[0]	0/[30]	0/[6]	0/[9]
Dipoles					
Bending[1]	0/[0]	4/[3]	0/[3]	0/[0]	0/[0]
Spectrometer[2]	0/[1]	0/[1]	0/[3]	1/[1]	0/[1]
Solenoid Magnets					
Compensation	0/[1]	0/[0]	0/[0]	0/[0]	0/[0]
Focusing	7/[0]	27/[27]	0/[0]	0/[0]	0/[0]

1) Bending magnets are defined to move the beam onto a new trajectory, ie,: not X and Y steering magnets.
2) Spectrometer magnets are defined to measure the beam energy and energy spread with a high degree of sensitivity.

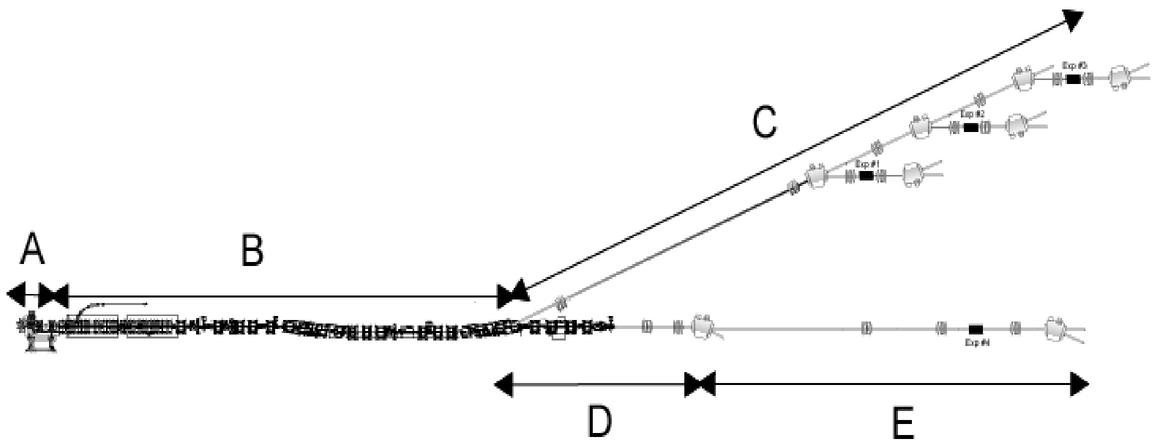

Figure 19. Relative positions of the NLCTA/ORION beamlines as referred to in Tables 9 and 10. Distances are not to scale.

3.6 Diagnostics

ORION operations and experiments will require instrumentation for measuring the position, energy, transverse size, length, spacing and intensity of electron bunches. In many cases where bunch characteristics are similar to those in the present NLCTA, standard beam position monitors (BPM), profile monitors, wire scanners, toroid intensity monitors, wall current monitors, bunch length monitors, bunch spacing monitors and Faraday cups will be used. There are special beam diagnostics for the photoinjector, and these were described in Section 3.2. There are also some special beam diagnostics in the final transfer lines leading to the experimental halls, which are required to resolve the ultra-short and/or low-emittance bunches prior to delivery to the users. Note from Table 2 that a large range of longitudinal and transverse emittances as well as bunch charge (pico to nano-Coulombs) will need to be measured at entry to the experimental halls. Table 10 summarizes the diagnostics presently installed in NLCTA and those anticipated for ORION by section, as designated in Figure 19.

Diagnostics for bunch charge, position, spot size, emittance, temporal length and energy spectrum will all be required to configure the machine for each user's needs. Diagnostic design is complicated by the desire to measure beam properties in two distinct ranges: (1) "Nominal charge, single bunch" mode with 0.25 to 4.0 nC charge, and (2) "Low charge, single bunch" mode with 2 to 20 pC charge. As such, some of the existing diagnostics at the NLCTA will need either modifications made to increase sensitivity, decrease response time, or both.

Temporally integrating diagnostics, such as the fluorescent screens and Faraday cups in NLCTA, view the thermionic source's long macropulse as a single bunch with ~100 nC charge. If one intends to also monitor the low-charge single bunch with these same diagnostics, the dynamic range requirement is severe at nearly 50dB. Variable attenuators can be used ahead of readout electronics for BPMs, toroids, and Faraday cups to expand the dynamic range provided that the readout electronics have sufficient sensitivity. Profile monitor cameras, however, will have to be augmented by intensified cameras to view the lowest charge bunches. Changing all charge injection device (CID) cameras presently installed and planned is too expensive, so it is proposed that only two or three key profile monitors be instrumented with intensified cameras, and that tune-up for the low-charge, single bunch mode begin with a tune-up with modest charge (e.g. 100 pC) that gives clear signals on all diagnostics, followed by a gradual reduction in charge (by reducing the radius of the laser spot on the cathode, holding the laser pulse energy constant so as to preserve the bunch focusing properties) while monitoring the intensified profile monitors and readjusting the focusing as needed.

Table 10. Presently Installed and [Anticipated] Diagnostics for ORION by Beamline Section.

	Source to Injector	**Injector to LE Hall Line**	**Low-Energy Hall Beamlines**	**LE Hall Line to HE Hall**	**High-Energy Hall Beamlines**
Figure 19 Location	**A**	**B**	**C**	**D**	**E**
BEAM ENERGY	7 MeV	7-67 MeV	7-67 MeV	67-350 MeV	67-350 MeV
Integrating Current Transformer	0/[1]	[3]	[11]	3	[6]
Faraday Cup	0/[2]	0	0	1	0
NLCTA Fluorescent Screen	0/[2]	1/[2]	[15]	4	[6]
NLCTA Wire Scanner	0	1	0	2	0
OTR Screen	[2]	[1]	[4]	0/[1]	[2]
NLCTA BPM	[1]	19	[18]	17	[8]
Pepper Pot	0/[1]	0/[1]	0	0	0
Bunch Length Monitor	[1]	1	0	0/[1]	0
Spectrometer	[1]	0/[1]	[6]	1	[1]

Emittance measurement by the quadrupole magnet scan/three-screen technique is sufficient for most cases once the beam energy is 50 MeV or higher. For the special high-density, low-energy beams produced by the rf photoinjector, however, emittance-mask techniques must be used. A "pepper pot" is planned for the ~1 meter beamline section immediately following the photoinjector to facilitate tune-up. A second pepper pot mask installed before the chicane is also desirable as it would give a convenient comparison measurement to use against the quadrupole scan technique.

Longitudinal phase space measurements are confined to energy spectrum in dispersive regions of the beamline, to beam current spectral content measurements at ceramic gaps, and to direct profile measurement with a "prompt" radiator (e.g. Cerenkov or optical transition radiation (OTR)) examined by a streak camera. Energy spectrum measurements are not confined to the ends of the experimenter's beamlines, where spectrometers are placed, but may also be done using the extraction "doglegs" at both the low-energy and high-energy extraction lines by placing profile monitors at suitable locations within the transport lines. High-frequency measurement of beam current spectra provides information about the approximate rms bunch length that is valuable in tuning the accelerating section phases and chicane dispersion, and desirable not only in the injector (as presently installed) but at the exit of the chicane, and again at the exit of the last accelerator section. Direct profile measurement by streak camera is envisaged during the source-commissioning phase to occur immediately after the photoinjector, and subsequently at the locations of the experiments themselves.

3.7 Conventional Facilities

3.7.1 Laser Rooms

The photoinjector's cathode is driven by the Ti:Sapphire laser described in Section 3.3. For ease of operation and maintenance, this laser is to be located outside the NLCTA concrete tunnel enclosure, but inside End Station B. A location on the north side of the enclosure and close to the photoinjector, as shown in Fig. 5, is presently planned. The room will be called Laser Room 1.

Purchase of a commercial laser room approximately 20' × 40' with an entry-exit vestibule is envisioned. It should be a Class 1000 clean room and air-conditioned to achieve temperature stability above the optical table at the level of ± 1/2°C. Laser power supply and racks are to be located outside and adjacent to the laser room. A rack for the laser control system will be in the clean room to minimize the path length for cabling to the laser table. The room will be shielded from electromagnetic noise. Installation of such a room could be in one complete package delivered by the vendor and dropped into place with the End Station B overhead crane.

A similar laser room as that for the photoinjector is required to house the lasers supporting the user experimental programs. This Laser Room 2 will be located near the Low Energy and High Energy Halls to reduce the light-path length (Fig. 1 and 5). This puts it outside the End Station B enclosure and will require more air-conditioning capacity to meet the temperature stability requirements, and a weather-tight building or shell needs to surround it. This laser room also must be to Class 1000 clean room standard and should be 20' × 40' with a vestibule.

3.7.2 Experimental Halls

Experimental modules will be assembled and surveyed onto standard girders in the Staging Area (Sec. 3.7.3). These units are then moved to the appropriate experimental hall during scheduled change-overs. Floor rails and linear bearings will be used to eliminate much of the final surveys in place. The Low Energy Hall (LEH) presently envisions three separate beam lines split off from the primary transfer line by means of DC dipole magnets. The separation between adjacent beamline centers is about 8 feet to facilitate experimental installation and maintenance.

The LEH is to be located adjacent to the East Wall of ESB and north of the NLCTA tunnel shielding enclosure. Its inside dimensions are presently set at 34' × 48' ×10' high resulting in ~1600 ft^2 of experimental area. The Hall will have one labyrinth-type entrance module complete with a personnel protection system (PPS) gate and one emergency exit physically separated from the entrance module. Experimental equipment installation and removal is either *via* an extra-wide labyrinth or *via* a separate, normally closed off entrance using a removable wall shielding block(s). The wall thickness of the LEH enclosure is 6 feet. The roof block thickness is 5 feet. Roof beams are not meant to be removed once installed by crane since they would support lighting, cable trays over the beam lines, 120V and 208V AC circuits with outlet boxes, and low-conductivity water (LCW) and gas lines. Wall blocks and roof blocks are patterned after the NLCTA staggered joint design shown in Figure 5 to prevent radiation escaping from cracks.

The High Energy Hall (HEH) is to be constructed adjacent to the east end of the NLCTA tunnel enclosure. The inside dimensions are roughly 15' wide × 65' long × 10' high resulting in about 1000 ft^2 and is adequate for one beamline. A future expansion of the HE Hall to about 5000 ft^2 (dimensions 39' wide × maximally 130' long × 10' high) is possible if the experimental program requires it. The HEH will have one labyrinth-type entrance module complete with a PPS gate and one emergency exit physically separated from the entrance module. Large experimental equipment installation/removal is *via* special removable concrete wall shielding blocks. The wall thickness of the HEH is 6 feet. The concrete roof blocks are 5 feet thick and are not intended to be removed once installed by crane. They will support lighting, cable-trays, 120V and 208V AC circuits, low-conductivity water (LCW) and gas lines. The concrete blocks are patterned after the NLCTA blocks.

Presently it is envisioned that electron beam will enter the HEH *via* one trajectory straight through the NLCTA east wall-plug which houses the NLCTA terminating beam stop. The penetration will be generated by perforation of the wall plug. A new terminating beam stop will be installed at the end of the beam line in the HEH with appropriate additional local shielding. A second penetration at an angle determined by the existing NLCTA spectrometer dipole magnet will also be made during the ORION civil construction phase. This hole will be filled with steel so as to maintain use of the spectrometer, but the penetration will be available if a future experimental program requires it.

3.7.3 Staging Area

The ORION Facility will require space for staging of experimental hardware before installation into the experimental halls. The present concept for the Staging Area is that it will occupy roughly 3500 square-feet in the planned SLAC Research Support Building to be constructed adjacent to and northeast of the NLCTA. The layout of this Staging Area is shown in Figure 20. It will consist of a high-bay assembly area (to be in a large common bay shared with the Experimental Facilities Dept.) with overhead crane coverage for experimental module preparation, a technician room and machine shop, four separate user lab/storage rooms, a clean room, and a Data Acquisition Room for users to monitor and run their experiments (Sec. 3.7.4).

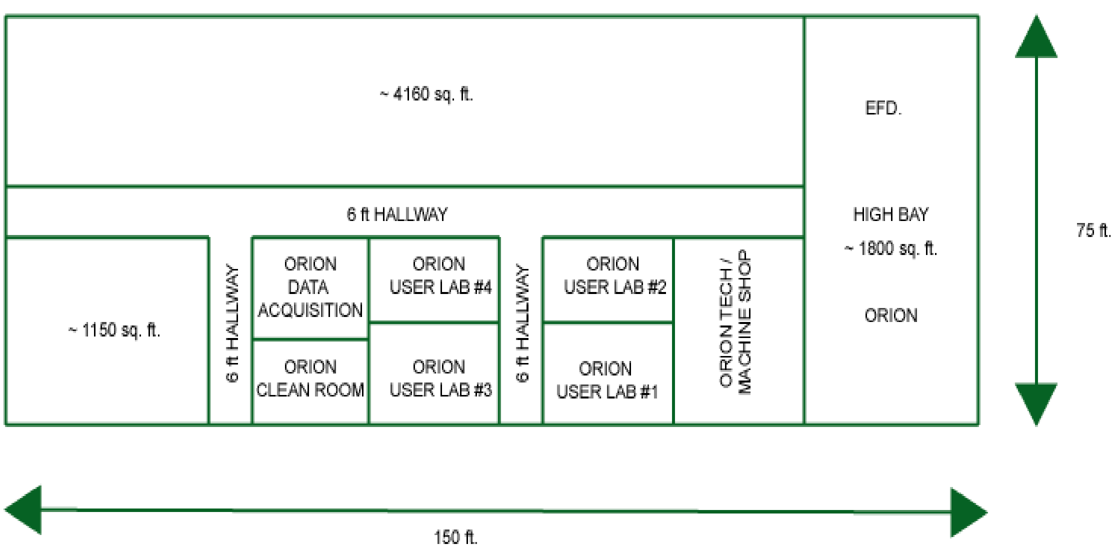

Figure 20. Drawing of the ORION Staging Area within the planned SLAC Research Support Building.

Also needed near the LEH/HEH is some modest amount of office space for the experimenters, be they Users or SLAC staff. This office space may also be in the same building as the Staging Area, but this is not yet decided.

The schedule for construction of the SLAC Research Support Building is not yet determined. Space for equipment preparation and storage will be needed during ORION construction. Presently, Accelerator Research Department B (ARDB) is using Building 102B which has a clean room with HEPA filters, an assembly space and is accessible by forklift. It is $35' \times 40' \equiv 1400$ ft^2 of which 200 ft^2 are dedicated to the clean room and 175 ft^2 are office space. A 200 ft^2 lab is adjacent to the main room. This building may be used during the ORION construction phase.

3.7.4 Data Acquisition Room

The NLCTA Control Room is presently dedicated to the operation and monitoring of the accelerator systems. It will be modified to include operator control of the complete ORION complex. ORION users will require a Data Acquisition Room (DAQ Room) close to the experimental halls and the user laser room for assembling the needed data acquisition computers and associated hardware for their experiments.

A 320 square-foot ($16' \times 20'$) room is presently envisioned for this purpose, located in the planned SLAC Research Support Building (Fig. 20), immediately northeast of the user laser room (Laser Room 2). This room is reserved specifically for users setting up or attending running experiments in the halls; data analysis and more general office usage are expected to take place in more distant user office space. Users will locate hardware specific for controlling and acquiring data from their experiments in this DAQ room, which will be equipped with two computer consoles for controlling beamline magnets immediately adjacent the users' experiments, and for reading beamline magnet configurations and diagnostics. The DAQ room will be connected to the experimental halls and laser rooms via dedicated signal-only cable trays, and will have access to the full complement of trigger and timing signals used in running the accelerator. Communication via telephone and intercom with the interior of the shielding enclosures, laser rooms, NLCTA main control room, and the Main Control Center of SLAC will be established.

3.7.5 Utilities and Services

The ORION Facility will require LCW water, compressed house air, 120V and 208V AC circuits and outlets, air-conditioning, specialty-gas lines, and lighting. The LCW needs are modest to cool the small dipole switcher magnets, spectrometer dipole magnets, the photoinjector, its laser and rf system. All the quadrupoles and corrector magnets have air-cooled solid conductor coils. End Station B and specifically NLCTA have enough AC and LCW capacity to satisfy all the envisioned ORION Facility requirements. Water headers will have to be brought into the LEH/HEH originating at the NLCTA main headers. The AC circuits will come from a spare breaker in the 3 MW substation south of ESB, which also serves NLCTA. Air-conditioning of Laser Room 1 and Laser Room 2 will have to be procured and should be located outside ESB. Air-conditioning, if any, of the LEH/HEH is still under discussion.

3.8 Control Systems

The ORION Facility control system will be integrated seamlessly into the present NLCTA control system, which is based on the SLC control system. The SLC VAX computer controls monitor the machine though a series of distributed microprocessors, which in turn control individual beam line components via CAMAC. The topology of the system is a logical star network with the Host machine coordinating geographically distributed slave microprocessor clusters. ORION will 'appear' to the SLC control system as one more microprocessor cluster. The ORION microprocessor cluster will be in parallel to NLCTA. The advantage of this arrangement is that software and hardware that have been extensively tested on all accelerators in the SLAC complex can be utilized.

The SLC control system is designed to allow the use of multiple independent control consoles. Full function control consoles consisting of a touch panel, graphics monitor and slew knobs exist in the NLCTA control room. Personal computer-based terminals capable of running X-windows are also available to use as a control system interface. Experimenters can use these terminals to run commercially available software, such as LabView, to control and record their individual experiments data. The SLC interface used by E-157 will be used to date stamp the ORION machine parameters to correlate experimental results to machine parameters.

3.9 Protection Systems

The protection systems are divided into three groups. The Beam Containment System (BCS) will insure that the confinement integrity of the beam line housing is not violated by large excursions of the beam from its nominal trajectory. The Personnel Protection System (PPS) will insure the safety of personnel in and around the NLCTA and ORION beam line housings by controlling access to the housings, by providing emergency-off controls, and by monitoring radiation levels via Beam Shutoff Ion Chambers (BSOIC). Any PPS or BCS violation will result in the inhibiting of redundant permissions to the associated systems. Finally, the Machine Protection System (MPS) will provide for the protection of beam line components and inhibit permissions to the associated systems in the event of a violation.

Because the ORION Facility is derived from modifications and additions to the existing NLCTA, the ORION protection systems will be extensions of these and integrated into the existing protection systems consistent with present ESH requirements at SLAC. The only novel introduction is the need to have the safety interlock system for the laser rooms and experimental halls designed to allow access to these when the two redundant beam stops are in place and particle beam is enabled in the radiation enclosures. Beam can only enter the experimental halls when the hall doors are interlocked shut and the redundant beam-stops are actively maintained in an open state. Also, for laser set-up and calibration, it is necessary to have access to the NLCTA enclosure and experimental halls when a laser is operational provided that appropriate personal protection equipment is in use.

The main X-band linac will be protected from catastrophic vacuum failure through the use of a commercially available fast acting vacuum isolation system. Individual detectors will be used to sense pressure increases on the transfer lines into HE and LE Halls. Slower, remotely controlled isolation valves will back up the fast valves. The location of the detectors and isolation valves will be chosen in such a way to protect the photoinjector along with the X-band linac sections from vacuum failure in either the LE or HE Halls.

4 Environment, Safety and Health

4.1 Overview

WORK IN PROGRESS:
THE TEXT IN THIS ESH CHAPTER IS PRELIMINARY AND WILL BE REVIEWED AND REVISED TO MAKE IT CURRENT WITH PRESENT DOE AND SLAC POLICY.THIS IS ONLY A FIRST ATTEMPT TO DESCRIBE THE ESH ISSUES FOR THE ORION PROJECT.

SLAC has various environment, safety, and health (ESH) programs already in place. From the ESH standpoint, the ORION modifications to the NLCTA do not present any significant new challenges. All of the anticipated hazards are ones that SLAC has successfully faced during its previous construction and experimental activities.

The SLAC programs in ESH will ensure that all aspects of the design, construction, installation, testing, and operational phases of the project are properly managed. As appropriate, the responsible SLAC safety committees, including the Safety Overview Committee, the Hazardous Experimental Equipment Committee, the Radiation Safety Committee, the Fire Protection Safety Committee, the Hoisting and Rigging Committee, the ALARA Committee, the Electrical Safety Committee, the Non-Ionizing Radiation Safety Committee, and the Earthquake Safety Committee will review and approve various aspects of the project. All aspects of the project will conform to the applicable DOE, national, and state codes and regulations, including those aspects of DOE 6430.1A that pertain to the ORION Project.

4.2 Fire Safety

The fire protection system, which will be a wet pipe design, will be in accordance with NFPA 13. SLAC subcontracts with the Palo Alto Fire Department to operate an on-site fire station and to provide emergency response services. The Palo Alto Fire Department also provides ongoing fire safety inspections of SLAC facilities, as well as training of personnel.

4.3 Radiation Safety

The design and operation of all facilities at SLAC are governed by the ALARA (as low as reasonably achievable) policy. Thus, SLAC has always maintained radiation dose limits below the maximum allowed by regulation.

Shielding for ORION will conform to the Design and Control section of DOE Order 5480.11, Section 9(J). The conceptual design of the shielding, described in Section 2.3.5, limits the dose equivalent in occupied areas to 1 mrem/year at the surface of the shield, under the same assumptions of beam losses as used in the NLCTA CDR (Ref. 3). However repetition rate limits will be employed for further dose reduction while the source of any unexpected beam loss are located and corrected. Activation of air, ground or beam line componenets will not be a significant radiological hazard. The dose at the SLAC site boundary, over 300 meters away, will be less than 0.1 mrem/year.

The Personnel Protection System (PPS) will insure the safety of personnel from radiation hazards in and around the ORION and NLCTA beam line housings by controlling access to the housings, by providing emergency shut-off controls, and by monitoring radiation levels via Beam Shutoff Ion Chambers (BSOIC). Any violation of the PPS will result in the inhibiting of redundant permissions to the associated systems. This will be accomplished through a system of electronically interlocked gates, lights, alarms, and operator displays and controls.

The Beam Containment System (BCS) will insure that the confinement integrity of the beam line housing is not violated by large excursions of the beam from the nominal trajectory. Any BCS violation will result in the inhibiting of redundant permissions to the associated systems.

In accordance with SLAC's implementation plan for DOE Order 5480.11 (Radiation Protection for Occupational Workers) and the SLAC Radiological Control Manual, all SLAC employees and any persons who work at the laboratory longer than one month must receive training in radiation fundamentals through General Employee Radiological Training. In addition, those workers and users whose assignments make it likely that they will receive a total occupational radiation dose larger than 100 mrem in one year receive more extensive radiation safety training and are classified as Radiation Workers.

4.4 Laser Safety

There are two laser areas planned for ORION, one to drive the photoinjector cathode and the second to be available for the users experimental programs. The current plans are to acquire two commercial laser rooms. The photoinjector laser room is to be located inside End Station B (ESB) on the north side of the NLCTA near the planned photoinjector. The laser room for the users is to be placed outside ESB, just to the east of the Low Energy Hall (LEH). This laser room will require an additional enclosure to protect it from the weather and help to achieve the required temperature stability.

The drive laser for the photoinjector cathode is envisioned to be a commercial Ti: Sapphire laser. The type of laser for the users' experimental programs is not yet determined, and it will change from time to time depending on the experimental needs and what kind of equipment the users will supply. Both lasers will be Class IV and, during operations, access to the laser rooms will be restricted to Qualified Laser Operators (QLO). Both Engineering and Administrative safety measures are required to ensure safe operation of these laser facilities. The planned ORION laser safety measures, which are summarized in this section, are expanded upon in Appendix A.

The potential hazards generated by the operation of these Class IV lasers are: 1) Exposure of the eyes and the skin to high energy laser light, resulting in cornea damage and skin burns, 2) Absorption of laser radiation can cause heating and potential combustion of materials which can then release toxic fumes, and 3) High Voltage Shock from exposure to voltage levels above 50V and possible exposure to ionizing radiation.

Administrative and Engineering measures are used to protect both untrained personnel and the trained QLOs. Both laser systems operate in two distinctly different environments. For the photoinjector drive laser it is the commercial laser room enclosure up to the NLCTA tunnel. For the user experimental facility it is the commercial laser room enclosure and the Low Energy Hall (LEH) or the High Energy Hall (HEH). The primary safety features of both laser systems are personnel training and access restrictions.

Personnel working on or operating these lasers will have to undergo training as described in more detail in Appendix B. Specifically, the laser operators will have to have read and understood the "American National Standards for the Safe Use of Lasers"; also, the chapter on "Laser Safety" in the SLAC ES&H Manual, and the pertinent section on laser safety in the laser manufacturers' literature for the specific laser. Further, the prospective laser operator must have passed the SLAC ES&H "Laser Worker Training Course" and must have fulfilled the SLAC Medical Department's requirements for Laser Operators. Since the lasers under consideration are Class IV, all laser operators must wear eye and skin protection suitable for the wavelength(s) anticipated when the lasers are on. There will be protective eyewear in the laser room and also just outside the "inner" door to the laser room.

Appendix A details the various engineering and administrative measures to be adopted during Normal Mode Operation and Bypass Mode Operation (for setup, laser alignment and maintenance) as well as the safety measures for transporting laser light.

4.5 High-Power RF Safety

The RF system of the ORION Facility will incorporate all the safety measures that are currently in place for high-power microwave systems at SLAC. All high-power microwave radiation will be confined in evacuated metallic waveguides. The source of high-power microwaves will be disabled by hardware interlock by any failure of the vacuum integrity of a waveguide.

4.6 Electrical Safety

It is SLAC policy that every necessary precaution is taken in the performance of work to protect all persons on the site from the risk of electrical shock and to minimize the probability of damage to property due to electrical accidents. This policy is implemented by assigning responsibility and adherence to the basic safety principles in the laboratory ESH manual, and by complying with regulations and procedures appropriate to each operation. The Laboratory provides appropriate electrical safety training courses for those workers who are likely to be exposed to electrical hazards.

The provisions for locking of ORION electrical systems during work will utilize SLAC's established procedures for lockout and tagout. All work will be performed in accordance with safe work practices and in accordance with OSHA 1910, Subpart S.

4.7 Construction

The line organization acting through the subcontract administrator has primary responsibility for overseeing safety compliance by construction subcontractors. This responsibility includes apprising subcontractors of SLAC and DOE safety criteria prior to construction, conducting periodic inspections of subcontractor construction areas to evaluate the quality of the subcontractor's safety compliance program, and receiving subcontractor accident reports and compiling information for reporting to DOE.

4.8 Emergency Preparedness

Like all experimental areas at SLAC, the ORION Facility will be designed, constructed, and operated in a manner that minimizes the risk of injury to personnel and property as a result of a natural disaster or other emergency situation. In the event of any abnormal condition, the interlock system will automatically shut the machine down until the situation is diagnosed and corrected. The formal emergency planning system described in the SLAC Emergency Preparedness Plan will insure a logical, organized, and efficient response to any emergency.

Due to the regional geography, one emergency situation likely to occur at SLAC is an earthquake. Buildings and structures at SLAC are designed to withstand the effects of a major earthquake. In addition, all mechanical components of the ORION Facility will be secured to protect persons working nearby. This will be assured by a review of the design and installation of any experimental equipment by the SLAC Earthquake Safety Committee. As with all activities at SLAC, operation of the ORION Facility will be covered by the SLAC Emergency Preparedness Plan.

4.9 Environmental Protection

Making room for some ORION components in End Station B and its exterior requires the removal of various technical items stored there. Materials to be moved will be surveyed and handled in a manner appropriate to the level of residual radioactivity present, if any. Construction and operation of the ORION Facility is not expected to cause any adverse impact on the groundwater. Preservation of groundwater quality will be ensured through the SLAC Groundwater Management Program in compliance with DOE Order 5400.1.

4.10 Hazardous Material Issues

In accordance with 29 CFR 1910.1200 (OSHA hazard communication standard), SLAC has developed a Hazard Communication Program. Under this program, SLAC directs department heads and group leaders to conduct regular inventories of hazardous materials, to make Material Safety Data Sheets (MSDS) available to all employees and users, to ensure appropriate labeling of hazardous materials, to train employees and users to identify and control hazards in the workplace, and to inform users, subcontractors, and temporary employees of the hazards that may be encountered at SLAC.

5 Administration

WORK IN PROGRESS:
TEXT FOR THESE SECTIONS IS BEING DRAFTED.

5.1 Project Management

5.2 Human Resources

5.3 Work Breakdown Structure and Cost Estimate

5.4 Schedule

5.5 Quality Assurance

Acknowledgements

The Technical Design Study for the ORION Advanced Accelerator Research Facility, presented in this document, is the result of the contributions of many physicists, engineers, designers and support staff at Stanford University, Stanford Linear Accelerator Center, University of California at Los Angeles, University of Southern California, and the Fermi National Accelerator Laboratory, working under the direction of the ORION project management team at SLAC.

This work is supported by the U.S. Department of Energy under contracts DE-AC03-76SFO0515 and DE-AC02-76CHO3000.

References

1. T. Tajima and J. Dawson, Phys. Rev. Letters. Vol. 43, 267 (1979).
2. See for example, the Proc. of the Ninth Advanced Accelerator Conference, Santa Fe, New Mexico, June 2000 (to be published by American Physical Society, New York).
3. NLCTA Conceptual Design Report, SLAC-Report-411, August 1993.
4. ORION: An Accelerator Research Facility at SLAC, SLAC internal report, July 1999 (included as an appendix in Ref. 5).
5. The ORION Workshop, February 23-25, 2000. See the workshop report at http://www-project.slac.stanford.edu/orion.
6. D.T. Palmer, "The Next Generation Photoinjector", Stanford Univ. Thesis, 1998.
7. E.R. Colby, "Design, Construction and Testing of a Radiofrequency Electron Photoinjector for the Next Generation Linear Collider", UCLA Thesis, 1997.
8. M. Ferrario et al, "HOMDYN Study for the LCLS Photoinjector", presented at the 2nd ICFA Advanced Accelerator Workshop on the Physics of High Brightness Beams, Nov. 9-12, 1999, Univ. of California, Los Angeles.
9. L. Serafini and J.B. Rosenzweig, "Envelope Analysis of Intense Relativistic Quasi-Laminar Beams in RF Photoinjectors: A Theory of Emittance Compensation", Phys. Rev. E, Vol. 55, pp.7565-7590 (1997).
10. J. Rosenzweig and E. Colby, "Charge and Wavelength Scaling of RF Photoinjector Designs" in the Proc. of the 1994 Adv. Accel. Conf., AIP Proc. No. 335, pp. 724-737 (1995).
11. L. Young et al, PARMELA version 3, LA-UR-96-1835, revised Dec. 4, 2000.
12. K. Halbach and R.F. Holsinger, "SUPERFISH - A Computer Program for Evaluation of RF Cavities with Cylindrical Symmetry", Particle Accelerators, Vol. 7, pp. 213-222 (1976). This program package also contains POISSON.
13. B. Carlsten and D.T. Palmer, "Enhanced Emittance Compensation in a High-Frequency RF Photoinjector using RF Radial Focusing", Nucl. Inst. Meth. A425, pp. 37-50 (1999).
14. S.G. Anderson and J.B. Rosenzweig, "Nonequilibrium Transverse Motion and Emittance Growth in Ultrarelativistic Space-Charge Dominated Beams", Phys. Rev. ST – Accel. and Beams, Vol. 3, 094201 (2000).
15. TRANSPORT, commercial version in AccelSoft PBO Lab 2.0, Gilespi Assoc ; accelsoft@ghga.com.
16. The path length difference for two particles is R_{56} times their relative momentum difference.
17. T. Katsouleas, Phys. Rev. A 33, 2056-2064 (1986).
18. J.B. Rosenzweig, B. Breizman, T. Katsouleas, and J.J. Su, Phys. Rev A 44, R6189-R6192 (1991).
19. N. Barov, et al, Phys. Rev. ST Accel. Beams 3, 011301 (2000).
20. W.J. Brown, et al, "Low Emittance Electron Beam Formation with a 17 GHz RF Gun", MIT, January 2001, submitted for publication.
21. A. Donaldson and R. Cassel, SLAC, private communication.
22. C. Adolphsen, SLAC, private communication.

Appendix A: ORION Laser Safety

As mentioned in prior sections there are two laser facilities planned for ORION, one to drive the photoinjector cathode and the second to be available for the **USERS** experimental programs. The current plans are to acquire two commercial laser rooms. The photoinjector laser room is to be located inside End Station B (ESB) on the north side of the NLCTA near the planned photoinjector. The laser room for the **USERS** is to be placed outside ESB, just to the east of the Low Energy Hall (LEH). This laser room will require an additional enclosure to protect it from the weather and help to achieve the required temperature stability.

The drive laser for the photoinjector cathode is envisioned to be a commercial Ti: Sapphire laser. The type of laser for the **USERS'** experimental programs is not determined yet, and it will change from time to time depending on the experimental needs and what kind of equipment the **USERS** will supply. Both lasers will be Class IV and, during operations, access to the laser rooms will be restricted to **Qualified Laser Operators (QLO).** Both Engineering and Administrative safety measures are required to ensure safe operation of these laser facilities.

A.1 Identification of Potential Hazards

The potential hazards generated by the operation of these Class IV lasers are:

- Exposure of the eyes and the skin to high energy laser light, resulting in cornea damage and skin burns. Exposure can be of a direct nature, which includes specular reflections of high power. It can also be of an indirect nature, which refers to high power diffuse reflections. Maximum permissible exposure (MPE) for skin is $1.05 W/cm^2$, whereas the MPE for eyes is only $15.8 \mu W/cm^2$. Also, exposure of the eyes to a Class IIIA CW helium-neon (HeNe) alignment laser, often used in laser rooms, is a potential hazard.
- Absorption of laser radiation can cause heating and potential combustion of materials, which can then release toxic fumes (particularly at power levels above $2 W/cm^2$).
- High Voltage Shock from exposure to voltage levels above 50V and possible exposure to ionizing radiation. Such electrical shock exposures can occur during maintenance or repair operations when protective covers are removed to allow access to active electrical components. Since these lasers are commercial products and are manufactured to be safe from hazards when operated in accordance with the manufacturer's operations safety manual, and since only **QLOs** or the manufacturer's representative are authorized to perform the kind of work, these hazards are not dealt with further in this document.

A.2 Laser Performance Specifications

(A) Drive Laser

The specifications for the drive laser for the photoinjector are:

• Wavelength:	___	nanometers
• Pulse energy:	___	joules
• Pulse length:	___	nanoseconds
• Repetition rate:	___	Hz
• Beam diameter (area) at laser exit:	___	*mm* (___*mm*^{2})

This laser is an ANSI Class IV System, both with respect to average output power and single pulse energy.

(B) User Experimental Facility Laser

The specifications for the laser for the USER experimental facilities are:

• Wavelength:	___	nanometers
• Pulse energy:	___	Joules
• Pulse length:	___	nanoseconds
• Repetition rate:	___	Hz
• Beam diameter (area) at laser exit:	___	*mm* (___*mm*^{2})

This laser is an ANSI Class IV System, both with respect to average output power and single pulse energy.

A.3 Measures for Protecting Against Laser Radiation Hazards

Administrative and Engineering measures are used to protect both untrained personnel and the trained **Qualified Laser Operators (QLO)**. Both laser systems operate in two distinctly different environments. For the photoinjector drive laser it is the commercial laser room enclosure up to the NLCTA tunnel. For the **USER** Experimental Facility it is the commercial laser room enclosure and the Low Energy Hall (LEH) or the High Energy Hall (HEH).

Administrative Safety Provisions

The primary safety features of both laser systems are personnel training and access restrictions.

Training

Personnel working on or operating these lasers will have to undergo training as described in more detail in Appendix B. Specifically, the laser operators will have to have read and understood the "American National Standards for the Safe Use of Lasers"; also, the chapter on "Laser Safety" in the SLAC ES&H Manual, and the pertinent section on laser safety in the laser manufacturers' literature for the specific laser. Further, the prospective laser operator must have passed the SLAC ES&H "Laser Worker Training Course" and must have fulfilled the SLAC Medical Department's requirements for Laser Operators. Since the lasers under consideration are Class IV, all laser operators must wear eye and skin protection suitable for the wavelength(s) anticipated when the lasers are on. There will be protective eyewear in the laser room and also just outside the "inner" door to the laser room.

A.3.1 Normal Mode Operation

Engineering Safety Provisions

In the Normal Mode of Operation, the NLCTA tunnel **Personnel Protection System (PPS)** is in the **"NO ACCESS"** mode and the drive laser is permitted to operate and deliver laser light to the tunnel. During this mode of operation personnel are prevented by the PPS from occupying the tunnel. When the PPS mode is set to "**CONTROLLED ACCESS"** or **"ACCESS PERMITTED"** to allow entry into the tunnel, the laser beam will be turned off by the automatic closure of the laser safety stopper(s)/shutter(s) located at either the exit of the laser housing or at the exit from the laser room/entrance into the laser optical transport system to the tunnel. The yet-to-be built LEH and HEH will have PPS entry modules similar to the ones in NLCTA. Entry conditions relative to the **USER** laser "Normal Mode Operation" will be the same as for the photoinjector drive laser.

The laser safety stopper/shutter can be opened when the tunnel or halls are in the "NO ACCESS" mode with the area "Search Reset" activated.

Administrative Safety Provisions

All components of each commercial laser system are located in their respective commercial laser rooms. Entry into each laser room is to be via a vestibule. Consequently, there will be an "outer door" through which to enter the vestibule and an "inner door" through which to enter the laser room. The "outer door" will not be interlocked, but only **QLOs** will have access to the keys. Emergency entry into the vestibule can be obtained using an "Emergency Key" located in a crash box with a breakable glass cover. The safety stopper(s) will not be inserted or hazards turned off until the "inner door" is opened.

The "inner door" will not be keyed and the knobset is "free turning" on both sides. This door will be interlocked with redundant closed sensing microswitches. The microswitches can be "bypassed" from both sides, for authorized entry/exit. When the door is opened in the bypassed condition, the laser safety stopper enables, and the hazard enables are not disrupted. The "inner door" has a timed controlled entry feature. When the entry bypass key switch is turned, the bypass will last for 30 seconds. If the inner door is not opened for entry or exit within 30 seconds, the bypass will be removed. After an entry or exit is successfully completed, the bypass will be removed within another 30 seconds from when the door is closed. If this door is opened without being "bypassed," the safety stopper(s) will go "in" and the laser high voltage will be shut off and the hazards will turn off.

There will be a laser PPS status panel on both sides of the inner door. The panels will have the aforementioned timed controlled entry keyed switch. The panels will show the following status conditions:

(a) Laser shutter “enable” and “out”
(b) Laser transport safety stopper (“enable”, “in” and “out”)
(c) Laser power supply “on”
(d) Entry Mode (permitted, time controlled, no entry)
(e) Timed bypass switch (“not bypassed”, “bypassed”)
(f) Outer Door Emergency Entry Key Interlock
(g) Inner Door (“bypassed” and “not bypassed” and “closed”)
(h) UH Vacuum O.K. (transport line)

Additional Engineering Safety Provisions

There will be a battery powered emergency light in each laser room. There will be at least three emergency AC crash off buttons in each laser room, at least one at each wall. Activating these buttons will turn off all power in each laser room including the laser power supplies. The emergency lights will turn on automatically.

The laser rooms will have smoke detectors and fire sprinkling system.

Additional Administrative Safety Provisions

The laser room “outside door” may only be opened by keys, the distribution of which is controlled by the SLAC Laser Safety Officer and only to **QLOs.** No one is allowed to lend their key to another person. There is a fire extinguisher in each laser room. There is at least one telephone in each laser room. There is a First Aid Kit accessible, either in the laser room or in the adjacent vestibule.

A.3.2 Laser Optical Transport System to Tunnel

The laser optical transport systems will be constructed such that flanged vacuum chamber connections are either not accessible between the laser room and the point of entry through the shielding wall (gun laser transport), or they will have padlocked protective covers which will require a key to open.

A second option is to have the transport system under vacuum (<0.5 atm) and interlocked with a pressure switch to insure vacuum integrity. The line must be under vacuum for the “External Interlock” to be made up. Should this interlock be tripped, the laser safety stopper(s) will block the laser light from entering the optical transport line. The NLCTA beam line chamber in the photoinjector region is also part of the External Interlock. The beam pipe must be under vacuum for the interlock to be made up. Any vacuum system entry in the photoinjector region will trip the interlock and insert the safety stopper(s) in the laser room.

A decision between these two options will be made at a later date.

A.3.3 Bypass Mode Operation

The PPS system includes a bypass mode needed for initial setup, general laser beam alignment checks, and maintenance. When in this mode, only **QLOs** are permitted in the NLCTA tunnel, the LEH and the HEH. This mode can be activated only by the ORION Laser Safety Officer with the use of a special PPS key which controls the TRANSPORT OVERRIDE ON THE TRANSPORT STOPPER CONTROL panel. This key cannot be released to anyone else. However, in case of absence, the ORION Laser Safety Officer can appoint another person with appropriate qualifications to assume the duties and become the interim ORION Laser Safety Officer. When this mode is activated the laser safety stopper(s) can be withdrawn thereby unblocking the optical transport line while the NLCTA tunnel or the LEH/HEH are in **CONTROLLED ACCESS** mode. A pair of redundant microswitches on each of the tunnel access/doors will trip off the laser high voltage if the Control Access condition is accidentally or forcefully violated. This is the only engineering control left, all others are bypassed and only administrative procedures are left.

Administrative Measures for Bypass Mode

Standard Laser Safety Warning Signs will be posted at the NLCTA tunnel entrances and/or at the LEH/HEH hall entrance gates.

In this mode, all **QLOs** entering the tunnel or halls must wear eye protection appropriate for the expected laser wavelength(s) and must wear it while in the tunnel and while the laser high voltage enable key is in the key switch on the laser.

Appropriate skin protection, such as laboratory coats, sleeve extensions, and gloves must be worn when handling optics located in the laser beam path.

Appendix B: Authorization for ORION Laser Operator

Operator Name (print): ________________________________Date: _________________

In Emergency Contact: Name: ___________________________Tel: (____)______-_______

Read this form, initial boxes that apply, and sign below.

1. I have read and understood
   - ☐ American National Standards for the Safe Use of Lasers (ANSI Z136.1-1993)
   - ☐ Chapter 10, "Laser Safety" of the SLAC ES&H Manual
   - ☐ "Laser Safety for the ORION Laser" (this document) and all Appendices.

2. I have passed ES&H course #253 "Laser Worker Training" ☐ Date_________________________
3. SLAC Medical Dept. Requirements for Laser Operator have been met.

   Date of medical surveillance eye exam:____
   Facility where eye exam was performed:____
   Medical Dept. representative signs here:____

4. I have received training for the ORION laser systems, and been judged qualified to operate them.

   ORION Laser Person In Charge signs here:________________________Date:________________

5. I understand that the ORION lasers are Class IV lasers and ORION HeNe lasers may be Class IIIB lasers, and the associated radiation can be hazardous to eye and skin. I also understand that there are electrical and perhaps gas hazards associated with the equipment. I agree to abide by and to enforce the rules of the "Laser Safety for the ORION Laser" document.

Operator Signature:____Date:________________

We authorize____to be an ORION Laser Operator.

ORION Laser Safety Officer:____Date:________________

ORION Project Responsible Person:_____________________________________Date:________________

NLCTA Safety Officer:____Date:________________

SLAC Laser Safety Officer:____Date:________________